

# Time-Dependent Density-Functional Theory (TD-DFT) with DEMON2K: ASESMA Exercises



DEMON stands for *densité de Montréal*. For obvious reasons, the unofficial DEMON logo is a demon or devil, mostly just for fun. This is a picture of Jun Maekawa's devil which is one of the most famous origami devils.

Mark Earl CASIDA

*Laboratoire de Spectrométrie, Interactions et Chimie théorique (SITh), Département de Chimie Moléculaire (DCM, UMR CNRS/UGA 5250), Institut de Chimie Moléculaire de Grenoble (ICMG, FR2607), Université Grenoble Alpes (UGA) 301 rue de la Chimie, BP 53, F-38041 Grenoble Cedex 9, FRANCE*

*e-mail: mark.casida@univ-grenoble-alpes.fr*

Date of Publication: May 24, 2025 (MS 0.05)

# Contents

<b>1</b>	<b>Introduction</b>	<b>3</b>
1.1	Preface . . . . .	3
1.2	Molecular Orbital and Valence-Bond Theory . . . . .	4
1.3	Molecular Hydrogen, H <sub>2</sub> . . . . .	6
<b>2</b>	<b>Exercises</b>	<b>11</b>
2.1	Installation . . . . .	11
2.2	Running the Program . . . . .	13
2.3	Vertical Excitations . . . . .	15
2.3.1	Atomic Units . . . . .	15
2.3.2	Basis Sets . . . . .	16
2.3.3	Dissociation Energy . . . . .	24
2.3.4	Excited States . . . . .	27
<b>3</b>	<b>Answers</b>	<b>32</b>
3.1	Answers for Section 2.3 . . . . .	32
3.1.1	Bond Dissociation Energy . . . . .	32
3.1.2	Excitation Energies . . . . .	35

# Chapter 1

## Introduction

### 1.1 Preface

These hands-on lessons have been prepared for the African School on Electronic Structure Methods and Applications (ASESMA) that took place in Accra, Ghana, in June 2025.

ASESMA



The *nominal* objective is

“to learn a bit about how time-dependent (TD) density-functional theory (DFT) works”

in a program such as DEMON2K designed for molecules. But the *real* objective is

“to learn about static and nondynamical correlation as well as how chemical physicists think about molecules.”

TD,  
DFT,  
DEMON2K

Traditionally ASESMA has focused on solid-state physics using periodic quantum physics codes. Quantum chemistry codes for molecules share many of the same principles that underlie periodic codes but with some differences which are partly historical and partly due to an emphasis on solving different types of problems. Let us develop this a little more.

A distinction is sometimes made between chemical physics and physical chemistry. Both are at the interface between chemistry and physics and so it can be hard (and not necessarily even

desirable) to distinguish one from the other. Traditionally chemical physics was done in physics departments and physical chemistry was done in chemistry departments. However a perusal of the table of contents of the American Institute of Physics (AIP) *Journal of Chemical Physics* shows that many chemical physicists are chemistry department faculty. What is going on? I think that the best explanation was given by the Rowlinson [1] who simply pointed out that the mathematics of traditional physical chemistry was adequate for thermodynamics, kinetics, and ion transport, but was relatively elementary compared to the mathematics routinely used in quantum mechanics. Hence, although, quantum mechanics is clearly the best way to model molecules, such work was traditionally relegated to physics departments until sometime in the 1970s. During the 1970s in the USA, quantum mechanics became well-established in physical chemistry courses and theoretical chemical physicists were hired in chemistry departments to do quantum mechanics. We had, in fact, reached the state where there is very little difference between chemical physics and physical chemistry and the identity of these two terms is even recognized in the name of the journal *Physical Chemistry Chemical Physics* (PCCP) published by the Royal Society of Chemistry.

AIP

PCCP

What distinction remains between chemical physics and physical chemistry might best be answered by the somewhat flippant answer of a graduate student to whom I had posed the question of the difference when I was looking for an appropriate school for graduate studies:

“The difference between the two is whether you do the fun part first or save it for last.”

Of course, he did not specify which part is the fun part (and I am sure that varies from person to person!) On a more serious note, chemistry is traditionally centered on chemical reactions. As such it is primarily concerned about how atoms move, with the behavior of electrons in molecules as a secondary concern which can help understand chemical reactivity. In contrast, physicists seem less concerned with chemical reactions and more interested in the properties of molecules which are often determined by what the electrons do when perturbed by (possibly time-dependent) electronic or magnetic fields. (To be fair, it should be pointed out that chemists make heavy use of the physical properties of molecules in order to confirm that they have indeed synthesized their target product!)

*Our purpose in these exercises is to explore strong correlation problems where a single determinantal (SDET) wave function is not enough.* Such problems are omnipresent in describing excited states in molecules but are also important for describing ground state potential energy surfaces (PESs) or, as we will often focus on diatomics, potential energy curves (PECs). As a rule, our focus will be on multideterminantal (MDET) wave functions. We will also focus on simple systems—notably  $H_2$ —and use the freely downloadable executable of DEMON2K which can easily be run on any personal computer running LINUX. In this way, we hope that the student will continue to experiment and to learn from DEMON2K, even after this ASESMA meeting.

SDET

PES,  
PEC  
MDET

## 1.2 Molecular Orbital and Valence-Bond Theory

Let us explore some of the more delicate differences between (solid-state) physics and (quantum) chemistry. These differences are important because they reflect different thought processes motivated both by historical differences and by differences in how mental models are used in these two closely-related fields.

It has frequently been remarked that physics uses plane-wave basis sets while chemistry uses atom centered basis sets. This corresponds to the difference between three types of ideal bonding recognized by chemists. The first type is metallic bonding where the conduction electrons are free to move in the field of ions in a metal. This may be approximated by the homogeneous electron gas

HEG,  
jellium

(HEG, also known as “jellium”), which is the old particle-in-a-box model with a uniform positive background to keep the system neutral and including electron correlation. Minimizing the jellium energy leads to a conduction electron density remarkably close to that of sodium metal, making sodium the closest real metal to the HEG.

Long ago, chemists developed an empirical model of two-electron bonding. This was further codified by the use of Lewis dot structures (LDSs) [2]. Note that we will use this term, even when not using dots to represent electrons. Hence  $[:N::N:]$ ,  $[:N\equiv N:]$ , and  $[N\equiv N]$  will all be called LDSs. (We will often put square brackets around our LDSs, though this is not a usual practice in chemistry.) As Lewis noted, this works equally well for describing covalent bonding and ionic bonding because ionic bonds are just extremely polar covalent bonds. LDSs are so deeply ingrained into chemical thinking that it is virtually impossible to work on, say, problems in organic electronics without knowing how to draw the LDSs of the molecules in the study.

LDS

Of course, metallic, covalent, and ionic bonding are just ideal cases. As emphasized, for example, by van Arkel’s triangle [3, 4], all real bonds have mixed character. This is further emphasized by applications of the electron localization function (ELF) to lithium clusters [5]. The ELF uses concepts from DFT to reveal electron pairs in molecules. The ELF is localized between atoms for covalent bonds. It also reveals nonbonding lone pair electrons. However lithium clusters,  $Li_n$ , are expected to form a covalent bond for the dimer and to gradually show metallic bonding as  $n$  increases. In fact, the ELF shows that for many lithium clusters, the electron pairs are actually located in the interstices between groups of atoms, rather than as bonds and lone pairs. This, apparently is what metallic bonding looks like according to ELF.

ELF

The advent of quantum mechanics made it urgent to be able to describe bonding in molecules. Just one year after the publication of Schrödinger’s famous paper [6, 7], Heitler and London published a paper which contained the valence-bond (VB) definition of the chemical in  $H_2$  [8]. *This theory is all about spin coupling!* But let us proceed without equations for now. Heitler and London proposed that the wave function for  $H_2$  could be written in two possible ways with one electron of each spin in an  $s$  atomic orbital (AO) on each atom, corresponding to the resonance structure  $[H\uparrow\downarrow H \leftrightarrow H\downarrow\uparrow H]$ . This provided a qualitatively correct description of bonding and greatly pleased chemists who could see the electron pair bond of  $[H-H]$ . In fact, the resonance structures are identified with  $[H-H]$  in VB theory but dissociate into the proper atomic states at long bond distance.

AO

Linus Pauling [9] began his career at the California Institute of Technology with the intention of using quantum mechanics to describe all of chemistry. As he was using VB theory, the wave function of  $H_2$  was

$$\Psi = C_{\uparrow\downarrow}\Psi[H\uparrow\downarrow H] + C_{\downarrow\uparrow}\Psi[H\downarrow\uparrow H], \quad (1.1)$$

so that the energy was (assuming real-valued wave functions),

$$E = \langle\Psi|\hat{H}|\Psi\rangle = |C_{\uparrow\downarrow}|^2\langle\Psi[H\uparrow\downarrow H]|\hat{H}|\Psi[H\uparrow\downarrow H]\rangle + 2C_{\uparrow\downarrow}C_{\downarrow\uparrow}\langle\Psi[H\uparrow\downarrow H]|\hat{H}|\Psi[H\downarrow\uparrow H]\rangle + |C_{\downarrow\uparrow}|^2\langle\Psi[H\downarrow\uparrow H]|\hat{H}|\Psi[H\downarrow\uparrow H]\rangle. \quad (1.2)$$

However Pauling and his student George W. Wheland [10, 11, 12] were not only interested in quantitative calculations but also in communicating useful concepts that chemists could use to understand chemical structure and reactivity. In so doing, they took the VB model and described it diagrammatically by using resonance structures. In so doing, they did a slight disservice by simplifying the energy expression to,

$$E = \langle\Psi|\hat{H}|\Psi\rangle \approx |C_{\uparrow\downarrow}|^2\langle\Psi[H\uparrow\downarrow H]|\hat{H}|\Psi[H\uparrow\downarrow H]\rangle + |C_{\downarrow\uparrow}|^2\langle\Psi[H\downarrow\uparrow H]|\hat{H}|\Psi[H\downarrow\uparrow H]\rangle, \quad (1.3)$$

in their verbal descriptions. Wheland struggled to make the resonance concept crystal clear:

“the newer concepts can be made clearer with the aid of an analogy. A mule is a hybrid between a horse and a donkey. This does not mean that some mules are horses and the rest are donkeys, nor does it mean that a given mule is a horse part of the time and a donkey the rest of the time. Instead, it means that a mule is a new kind of animal, neither horse nor donkey, but intermediate between the two and partaking to some extent of the character of each. Similarly, the theories of intermediate stages and of mesomerism picture the benzene molecule as having a *hybrid* structure, not identical with either of the Kekulé structures, but intermediate between them.” — p. 3 of Ref. [10].

Judging from his use of different analogies at different times [12], Wheland was probably not completely happy with any of these explanations. Certainly the “mule = donkey + horse” explanation of resonance in chemistry is wrong because expectation values necessarily contain cross terms.

Molecular orbital (MO) theory was a competing theory for describing the electronic structure of molecules. MOs were typically constructed as linear combinations of atomic orbitals, thereby defining the LCAO approximation. Because MO theory used a SDET of orthonormal MOs, it was much easier for doing calculations than was VB theory which required the use of linear combinations of several SDETs of nonorthonormal AOs. Furthermore, the number of possible resonance structures that needed to be taken into account in VB theory seemed to explode in going to large molecules (i.e., the  $N!$  problem of VB theory). For example, VB theory must also include the ionic structures  $[\text{H}:\text{H}^+ \leftrightarrow \text{H}^+:\text{H}]$  in the case of  $\text{H}_2$ . This is why almost all calculations (including DFT calculations!) are done these days using MO theory.

MO,  
LCAO

However VB theory is still very much alive as anyone who has a General Chemistry textbook can attest. While it is true that MO theory is invariably used to describe the electronic structure of diatomics (and the paramagnetism of  $\text{O}_2$  is heralded as a victory of MO over VB theory even though Wheland showed how VB theory also predicts paramagnetism [13]), VB hybrid orbitals and bonding concepts are also introduced and resonance structures abound! Moreover, unbeknownst to most chemists, the highly mathematical subject of spin-coupling underlies their VB theory (e.g., [14]) and the only way to explain why benzene resonance structures whose  $\pi$  bonds cross are forbidden is because these structures are actually based upon the Rumer method of spin coupling [15].

World War II is often used as an arbitrary division between classical VB and modern VB theory. With this division the Coulson-Fischer proof of the equivalence of VB and MO configuration interaction (CI) theory falls just barely into the category of modern VB theory [16]. Modern VB theory has overcome many of the old problems of classical VB theory and is now roughly competitive with MO theory [17, 18, 19]. This is not the place to go into modern VB theory. *However VB ideas are extremely useful for the analysis of the dissociation of the ground and excited states of  $\text{H}_2$ .*

CI

## 1.3 Molecular Hydrogen, $\text{H}_2$

The simplest molecule is  $\text{H}_2^+$  but the simplest neutral molecule is  $\text{H}_2$  for which the potential energy curves are well-known. For example, the following figure is from Ref. [20, 21]:



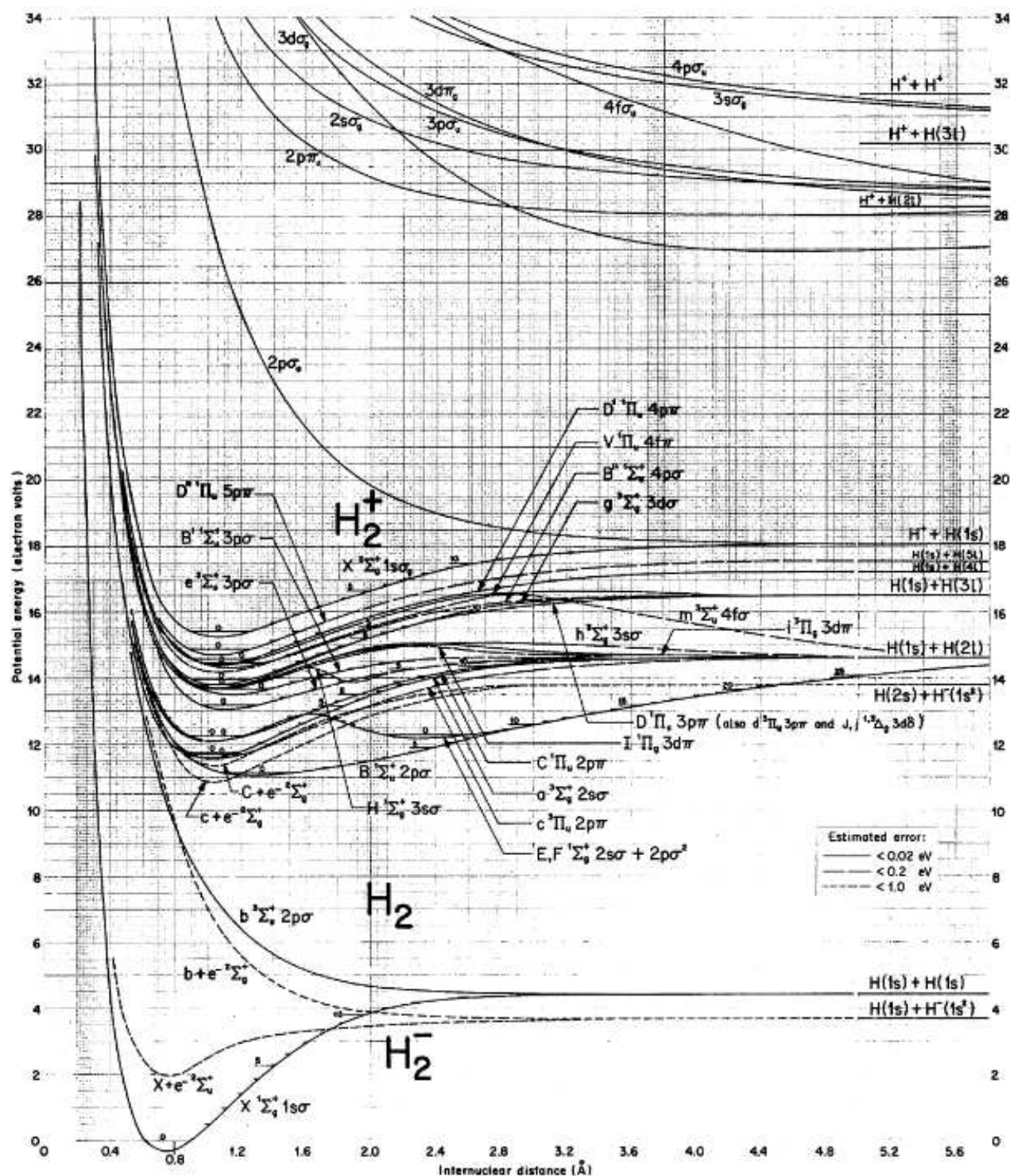


FIG. 2. Potential-Energy Curves for  $H_2^+$ ,  $H_2$ , and  $H_2^-$   
 A large-scale pullout of this drawing appears at the front of this issue  
 In general  $1s\sigma$  has been omitted from state designations in order to save space

Note that this graph contains curves not only for  $H_2$  but also curves for  $H_2^-$  and for  $H_2^+$ . In general, the more electrons, the lower the energy.

Because of time limitations, we will not try to calculate all of the PECs but will instead focus on the ground state  $X^1\Sigma_g$ , the first triplet state  $a^3\Sigma_u$ , and two excited states  $B^1\Sigma_u$  and  $E, F^1\Sigma_g$ . We

will be especially interested in the shapes of the PECs and in how  $\text{H}_2$  dissociates for the different states. From the graph, the dissociation of the  $X^1\Sigma_g$  and  $a^3\Sigma_u$  states is to form  $[\text{H}\uparrow\downarrow\text{H} \leftrightarrow \text{H}\downarrow\uparrow\text{H}]$ , while the dissociation of the  $B^1\Sigma_u$  and  $E, F^1\Sigma_g$  states is to form  $[\text{H}:\text{H}^+ \leftrightarrow \text{H}^+:\text{H}]$ . We will just use the local density approximation (LDA) in its Vosko-Wilk-Nusair (VWN) parameterization [22] and only moderately-sized basis sets. LDA,  
VWN

Accurate PECs from the work of Kołos and Wolniewicz [23, 24, 25, 26, 27, 28, 29, 30, 31, 32] are given in the following table (obtained by digitizing Fig. 1 of Ref. [33]):

$R/\text{bohr}$	Potential Energy Curves/Ha			
	$X^1\Sigma$	$b^2\Sigma_u$	$B^1\Sigma_u$	$E, F^1\Sigma_g$
0.0				
0.1				
0.2				
0.3				
0.4				
0.5	0.45307			
0.6	0.22525			
0.7	0.07491			
0.8	-0.02493			
0.9	-0.08672	0.44505		
1.0	-0.12603	0.38554	0.41482	
1.1	-0.14969	0.32183	0.37067	0.38259
1.2	-0.16419	0.28854	0.33657	0.34815
1.3	-0.17129	0.24684	0.31334	0.32451
<b>1.4</b>	<b>-0.17404</b>	<b>0.22004</b>	<b>0.29425</b>	<b>0.30936</b>
1.5	-0.17254	0.19490	0.28030	0.29829
1.6	-0.16849	0.17150	0.26977	0.29100
1.7	-0.16240	0.15029	0.26169	0.28650
1.8	-0.15503	0.13191	0.25565	0.28408
1.9	-0.14695	0.11617	0.25131	0.28335
2.0	-0.13836	0.10254	0.24815	0.28378
2.1	-0.12928	0.09088	0.24637	0.28518
2.2	-0.12027	0.08002	0.24467	0.28737
2.3	-0.11155	0.07028	0.24382	0.29000
2.4	-0.10266	0.06237	0.24356	0.29297
2.5	-0.09417	0.05439	0.24364	0.29626
2.6	-0.08610	0.04761	0.24383	0.29956
2.7	-0.07840	0.04179	0.24457	0.30285
2.8	-0.07113	0.03654	0.24547	0.30582
2.9	-0.06423	0.03181	0.24648	0.30835
3.0	-0.05778	0.02769	0.24769	0.31025

$R_e = 1.4 \text{ bohr}$

$D_e = 0.17404 \text{ Ha}$

triplet excitation energy  $E(b^2\Sigma_u) - E(X^1\Sigma) = 0.39408 \text{ Ha}$

singlet excitation energy  $E(B^1\Sigma_u) - E(X^1\Sigma) = 0.46829 \text{ Ha}$

spin multiplet splitting  $E(B^1\Sigma_u) - E(b^2\Sigma_u) = 0.07421 \text{ Ha}$

$E(E, F^1\Sigma_g) - E(X^1\Sigma) = 0.48340 \text{ Ha}$



$R/\text{bohr}$	Potential Energy Curves/Ha			
	$X^1\Sigma$	$b^2\Sigma_u$	$B^1\Sigma_u$	$E, F^1\Sigma_g$
3.1	-0.05177	0.02409	0.24900	0.31094
3.2	-0.04621	0.02093	0.25041	0.31021
3.3	-0.04114	0.01818	0.25197	0.30777
3.4	-0.03646	0.01573	0.25361	0.30480
3.5	-0.03225	0.01349	0.25532	0.30152
3.6	-0.02844	0.01157	0.25715	0.29820
3.7	-0.02517	0.01000	0.25905	0.29522
3.8	-0.02209	0.00862	0.26093	0.29264
3.9	-0.01940	0.00735	0.26276	0.29054
4.0	-0.01698	0.00629	0.26464	0.28888
4.1	-0.01484	0.00528	0.26675	0.28761
4.2	-0.01294	0.00435	0.26878	0.28675
4.3	-0.01125	0.00371	0.27094	0.28625
4.4	-0.00977	0.00317	0.27296	0.28616
4.5	-0.00857	0.00257	0.27508	0.28631
4.6	-0.00753	0.00216	0.27701	0.28682
4.7	-0.00650	0.00166	0.27923	0.28740
4.8	-0.00564	0.00136	0.28139	0.28824
4.9	-0.00499	0.00116	0.28349	0.28935
5.0	-0.00434	0.00090	0.28561	0.29056
5.1	-0.00384	0.00055	0.28769	0.29181
5.2	-0.00333	0.00039	0.28974	0.29328
5.3	-0.00322	0.00034	0.29180	0.29503
5.4	-0.00287	0.00014	0.29385	0.29689
5.5	-0.00282	-0.00006	0.29586	0.29868
5.6	-0.00281	-0.00011	0.29784	0.30049
5.7	-0.00269	-0.00019	0.29993	0.30343
5.8	-0.00245	-0.00037	0.30196	0.30430
5.9	-0.00237	-0.00039	0.30556	0.30611
6.0	-0.00237	-0.00017	0.30567	0.30793

$R/\text{bohr}$	Potential Energy Curves/Ha			
	$X^1\Sigma$	$b^2\Sigma_u$	$B^1\Sigma_u$	$E, F^1\Sigma_g$
6.1	-0.00237	0.00018	0.30944	0.30982
6.2	-0.00237	-0.00042	0.30955	0.31126
6.3	-0.00237	-0.00020	0.31137	0.31207
6.4	-0.00237	-0.00020	0.31321	0.31287
6.5	-0.00237	-0.00020	0.31510	0.31368
6.6	-0.00237	-0.00020	0.31685	0.31489
6.7	-0.00237	-0.00020	0.31870	0.31653
6.8	-0.00237	-0.00019	0.32043	0.31813
6.9	-0.00237	-0.00017	0.32211	0.31975
7.0	-0.00237	-0.00031	0.32382	0.32142
7.1	-0.00237	-0.00052	0.32546	0.32308
7.2	-0.00237	-0.00052	0.32702	0.32461
7.3	-0.00237	-0.00048	0.32861	0.32628
7.4	-0.00237	-0.00052	0.33024	0.32795
7.5	-0.00237	-0.00048	0.33177	0.32951
7.6	-0.00237	-0.00048	0.33331	0.33086
7.7	-0.00237	-0.00048	0.33477	0.33212
7.8	-0.00237	-0.00048	0.33632	0.33352
7.9	-0.00237	-0.00048	0.33773	0.33510
8.0	-0.00237	-0.00060	0.33913	0.33678

We will refer to these values as EXACT.

EXACT

# Chapter 2

## Exercises

### 2.1 Installation

This section is taken essentially verbatim from Workbook 1 [34, 35].

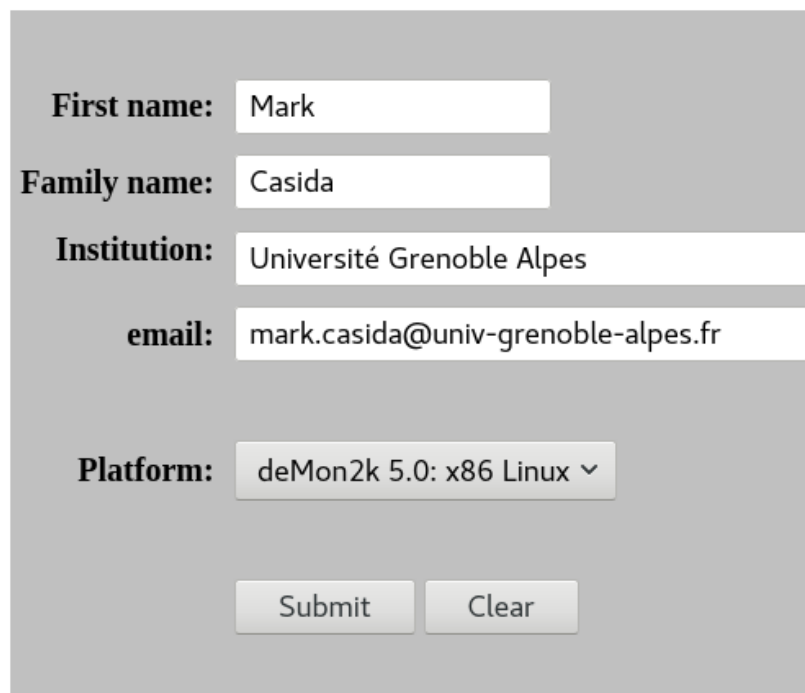
DEMON2K should run under most UNIX operating systems. If you do not have a computer running UNIX, it is possible to run UNIX on top of WINDOWS on a personal computer (PC) or on top of the APPLE operating system. An appendix in Workbook 1 explains how Nabila Oozeer installed UNIX on her Mac notebook without removing the APPLE operating system.

UNIX,  
WIN-  
DOWS,  
APPLE,  
PC

Let us assume that you have succeeded in finding or creating a UNIX environment. Let us see how you can install DEMON2K on your machine by looking at how I installed it on my machine. Specifically I installed a binary version on my portable computer which runs CENTOS LINUX. Installation involved several steps:

CENTOS,  
LINUX

1. Going to [http://www.demon-software.com/public\\_html/download/binary/download.html?](http://www.demon-software.com/public_html/download/binary/download.html?)
2. Filling in the form:



<b>First name:</b>	<input type="text" value="Mark"/>
<b>Family name:</b>	<input type="text" value="Casida"/>
<b>Institution:</b>	<input type="text" value="Université Grenoble Alpes"/>
<b>email:</b>	<input type="text" value="mark.casida@univ-grenoble-alpes.fr"/>
<b>Platform:</b>	<input type="text" value="deMon2k 5.0: x86 Linux"/>
<input type="button" value="Submit"/> <input type="button" value="Clear"/>	

3. Creating a suitable directory for unpacking:

```
/home/mcasida/ENGINEERING/workbook/deMon->ls
deMon2k.5.0.x86_linux.tgz
```

4. Changing to that directory and unpacking it:

```
> cd /home/mcasida/ENGINEERING/workbook/deMon
> gunzip deMon2k.5.0.x86_linux.tgz
> ls
deMon2k.5.0.x86_linux.tar
>tar xvf deMon2k.5.0.x86_linux.tar
AUXIS
BASIS
binary
ECPS
FFDS
MCPS
> ls
AUXIS  BASIS  binary  deMon2k.5.0.x86_linux.tar  ECPS  FFDS  MCPS
```

The executable is the file called `binary`. There are also several other files: `BASIS` contains a library of orbital basis sets, `AUXIS` contains a library of auxiliary basis sets for fitting the charge density and exchange correlation (xc) terms, `ECPS` and `MCPS` contain effective core potentials and model core potentials (two very similar concepts) respectively, and `FFDS` contains force field parameters for molecular modeling.

`BASIS`,  
`AUXIS`,  
`xc`, `ECPS`,  
`MCPS`,  
`FFDS`

5. Creating a simple input file `deMon.inp` containing:

```
TITLE 02 (Basis: GEN-A3*/6-311++G**)
MULTI 3
#
VXCTYPE VWN
#
PRINT MOS
VISUALIZATION MOLDEN FULL
#
# --- GEOMETRY ---
#
#
GEOMETRY CARTESIAN ANGSTROM
0      0.000000      0.000000      0.603500
0      0.000000      0.000000     -0.603500
```

This is a single point calculation for the  $\text{O}_2$  molecule in its triplet ground state using the LDA.

6. Run the program directly in the directory with the binary:

```

> ./binary < deMon.inp >& deMon.out
> ls
AUXIS  binary                                deMon.inp  deMon.mol  deMon.out  ECPS  MCPS
BASIS  deMon2k.5.0.x86_linux.tar  deMon.mem  deMon.new  deMon.rst  FFDS
> vi deMon.out

```

The program ran correctly, creating several additional files, including the main output in `deMon.out`, a restart file `deMon.rst`, one used for molecular visualization `deMon.mol`, and the files `deMon.meme` and `deMon.new`. The program seems to be working just fine.

## 2.2 Running the Program

This section is taken verbatim from Workbook 1 [34, 35].

Right now you have a directory (which I will call the `deMon_root` directory) which contains your executable, `BASIS` directory, `AUXIS` directory, etc. For various reasons, you do not want to run in the `deMon_root` directory. Instead, it is convenient to create a `SHELL` program (which I call `run.csh`) to run `DEMON2K` for you and do any clean up you might want to do afterwards. This section provides a simple example of how this is done.

`deMon_root`,  
`SHELL`,  
`run.csh`

Note that the ending `run.csh` indicates that this program is written in C `SHELL` (`csh`). Other options are possible, but I like C `SHELL`. My program is intended to be small and easily modifiable so that, once you understand it, you can adjust it to your own purposes and start to build your own `SHELL` programs.

`csh`

My program may be run in any directory of your account. It will look for a `DEMON2K` input file named `xxx.inp` in the same directory where “xxx” can be pretty much anything. Since `DEMON2K` always reads input from a file called `deMon.inp`, the file `xxx.inp` will have to be copied to `deMon.inp`. Also `run.csh` will have to copy the `DEMON2K` executable and any essential directories to the present directory. The job is then run. Once the job has finished, the output file `deMon.out` is renamed `xxx.out` (same “xxx” as for `xxx.inp`) and all the unimportant files are removed. In order to keep things simple, `run.csh` runs `DEMON2K` in foreground.

`deMon.inp`,  
`deMon.out`

Here is the contents of `run.csh` which I have placed in the directory `/home/mcasida/ENGINEERING/workbook/examples`.

```

#!/bin/csh
# The previous line indicates that this is a C-shell file
# -----
# Program to run deMon in the present working directory.
# To use: Create an input file with the name xxx.inp where
# xxx can be anything. Execute with
# /home/mcasida/ENGINEERING/workbook/examples/run.csh xxx
# The job runs interactively in foreground.
# -----
set xxx = $1
echo "Input file "$xxx.inp
set PWD = `pwd`
echo "The present working directory is "$PWD
set deMon_root = /home/mcasida/ENGINEERING/workbook/deMon # location of deMon files
echo "Using directories and executables from "$deMon_root

```



```

#
# copy essential files to the present working directory
#
cp $deMon_root/BASIS $PWD # copy the BASIS file to the run directory
cp $deMon_root/AUXIS $PWD # copy the AUXIS file to the run directory
cp $deMon_root/binary $PWD/deMon.x # copy the executable to the run directory
cp $xxx.inp deMon.inp
#
# run deMon
#
./deMon.x
#
# clean up
\rm BASIS
\rm AUXIS
mv deMon.out $xxx.out
\rm deMon.*
# -----
# End of file
# -----

```

Note that comments begin with the “number sign” (#) except for the first line in `run.csh` which tells my computer that this is a `csh` program. The program needs to be made executable:

```
> chmod ugo+x run.csh
```

Let us see how the program works. I have copied the input file from Sec. 2.1 to the directory `/HOME/MCASIDA/ENGINEERING/WORKBOOK/EXAMPLES/LESSON0` as the file `02.inp`. Here is a transcript of my session:

```

> ls
02.inp
> cat 02.inp
TITLE 02 (Basis: GEN-A3*/6-311++G**)
MULTI 3
#
VXCTYPE VWN
#
PRINT MOS
VISUALIZATION MOLDEN FULL
#
# --- GEOMETRY ---
#
#
GEOMETRY CARTESIAN ANGSTROM
0      0.000000      0.000000      0.603500
0      0.000000      0.000000     -0.603500
> /home/mcasida/ENGINEERING/workbook/examples/run.csh 02
Input file 02.inp

```

The present working directory is /home/mcasida/ENGINEERING/workbook/examples/Lesson0  
 Using directories and executables from /home/mcasida/ENGINEERING/workbook/deMon  
 > ls  
 02.inp 02.out

In addition to the input file 02.inp, I now have my output file 02.out but nothing else. This is enough to get us started.

## 2.3 Vertical Excitations

Let us start by examining the minimum energy geometry of H<sub>2</sub> and what the excited states look like at this geometry. This will allow us to discuss several aspects of multideterminantal (MDET) calculations.

MDET

### 2.3.1 Atomic Units

Before going any further, it is important to discuss units. We will be using Hartree atomic units for convenience. Hartree atomic units are based upon the Gaussian system of electromagnetic units where Maxwell's equations have the form,

$$\begin{aligned}
 \vec{\nabla} \cdot \vec{E} &= 4\pi\rho(\vec{r}) \\
 \vec{\nabla} \times \vec{E} &= -\frac{1}{c} \frac{\partial \vec{B}}{\partial t} \\
 \vec{\nabla} \cdot \vec{B} &= 0 \\
 \vec{\nabla} \times \vec{B} &= \frac{4\pi}{c} \vec{j}(\vec{r}) + \frac{1}{c} \frac{\partial \vec{E}}{\partial t}.
 \end{aligned} \tag{2.1}$$

This may be compared with Maxwell's equations in *Système internationale* (SI) units,

SI

$$\begin{aligned}
 \vec{\nabla} \cdot \vec{E} &= \frac{\rho(\vec{r})}{\epsilon_0} \\
 \vec{\nabla} \times \vec{E} &= -\frac{1}{c} \frac{\partial \vec{B}}{\partial t} \\
 \vec{\nabla} \cdot \vec{B} &= 0 \\
 \vec{\nabla} \times \vec{B} &= \mu_0 \vec{j}(\vec{r}) + \mu_0 \epsilon_0 \frac{\partial \vec{E}}{\partial t} \\
 \mu_0 \epsilon_0 &= \frac{1}{c^2}.
 \end{aligned} \tag{2.2}$$

The presence of  $\mu_0$  and  $\epsilon_0$  in SI units means that SI units actually have one more fundamental dimension than is the case in Gaussian units—hence the historical preference for Gaussian units in theoretical work. Furthermore charges and magnetic fields have different dimensionality in the two systems of units. This is easiest to see if we neglect the magnetic field ( $\vec{B} = \vec{0}$ ). Then Coulomb's law in Gaussian units is,

$$F = \frac{q_1 q_2}{r_{1,2}}, \tag{2.3}$$

and in SI units is,

$$F = \frac{Q_1 Q_2}{(4\pi\epsilon_0)r_{1,2}}. \tag{2.4}$$

Evidently,

$$Q = \sqrt{4\pi\epsilon_0}q, \quad (2.5)$$

for most of the applications that we are likely to encounter.

Hartree atomic units begin with the Gaussian system of electromagnetic units and set  $\hbar = m_e = e = 1$  atomic unit. In this system, the units of distance and energy are,

$$\begin{aligned} 1 \text{ bohr} &= a_0 = \frac{\hbar^2}{m_e e^2} = 0.529 \text{ \AA} \\ 1 \text{ hartree} &= 1 \text{ Ha} = E_h = \frac{\hbar^2}{m_e a_0^2} = 27.2 \text{ eV} = 219,000 \text{ cm}^{-1} = 628 \text{ kcal/mol}. \end{aligned} \quad (2.6)$$

(As a side note,  $c = 137.03599$  atomic units is curiously close to exactly 137.) *It is very important to realize that some programs use Rydberg atomic units.* These are the same as Hartree atomic units, except that the energy unit is the rydberg (Ry):  $1 \text{ Ha} = 2 \text{ Ry}$ ;  $1 \text{ Ry} = 0.5 \text{ Ha}$ . Ha, Ry

## 2.3.2 Basis Sets

This section is taken essentially verbatim from Workbook 1 [34, 35].

**LCAO approximation** It is well-known that the many-body problem cannot be solved exactly and so approximations are needed. However physicists (by which I generally mean solid-state physicists who are used to doing periodic calculations on metals and semiconductors) and chemists (by which I generally mean physical chemists/chemical physicists who are used to doing calculations on molecules) typically build their approximations based upon different physical pictures. For a physicist, the first approximation is that of an idealized metal where the wave functions of the conduction electrons are plane waves. These plane waves are delocalized over physical  $(x, y, z)$  space but localized in momentum space and lend themselves to Fourier transform methods. For a chemist, on the other hand, molecules are thought of as made up of atoms which interact to make bonding MOs, nonbonding MOs, and antibonding MOs. The simplest approximation is that each MO is the LCAO approximation. Although this is only a first approximation to more accurate descriptions of the electronic structure of molecules, it is still at the heart of much of chemical thinking. Each MO  $\psi_i$  is expanded in terms of AOs  $\chi_\mu$  as,

$$\begin{aligned} \psi_i(\vec{r}) &= \sum_{\mu} \chi_{\mu}(\vec{r}) C_{\mu,i} \\ \left( \psi_1(\vec{r}) \quad \psi_2(\vec{r}) \quad \cdots \psi_n(\vec{r}) \right) &= \left( \chi_1(\vec{r}) \quad \chi_2(\vec{r}) \quad \cdots \chi_m(\vec{r}) \right) \begin{bmatrix} C_{1,1} & C_{1,2} & \cdots & C_{1,n} \\ C_{2,1} & C_{2,2} & \cdots & C_{2,n} \\ \vdots & \vdots & \ddots & \vdots \\ C_{m,1} & C_{m,2} & \cdots & C_{m,n} \end{bmatrix}, \end{aligned} \quad (2.7)$$

where the  $C_{\mu,i}$  are referred to as MO coefficients. Notice how Latin indices are used for MOs and Greek indices are used for AOs. This is a very consistent practice throughout the Quantum Chemistry literature. Also capital Latin and Greek letters (such as  $\Psi$ ) are reserved for many-electron quantities while small Latin and Greek letters (such as  $\psi$ ) are reserved for 1-electron (e.g., MO) quantities, but there are some exceptions as capital letters are frequently used for matrices for historical reasons.

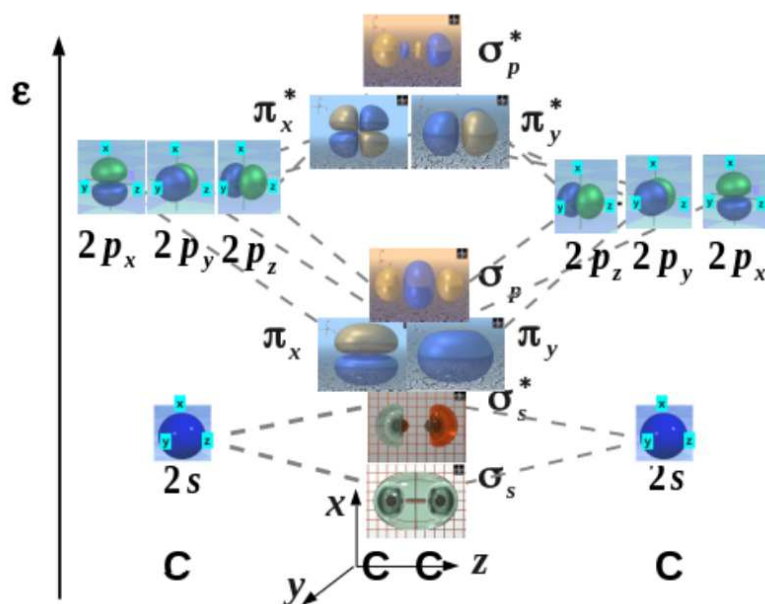


Figure 2.1: Part of the solution to last year’s final exam in the first-year course (CHI 131) that I teach. Notice how AOs with  $S > 0$  come together to create MOs with lower energy than the corresponding AOs (i.e., are bonding) while AOs with  $S < 0$  come together to create MOs with higher energy than the corresponding AOs (i.e., are antibonding).

Each AO is naturally enough centered on an atom (often referred to as a “center”). True AOs on any given center are orthonormal (or, more exactly, may be chosen to be orthonormal),

$$S_{\mu,\nu} = \langle \chi_\mu | \chi_\nu \rangle = \int \chi_\mu^*(\vec{r}) \chi_\nu(\vec{r}) d\vec{r} = \delta_{\mu,\nu} = \begin{cases} 1 & \text{if } \mu = \nu \\ 0 & \text{if } \mu \neq \nu \end{cases} . \quad (2.8)$$

However AOs from different atoms are *not* orthonormal and chemists are used to visualizing how the AOs interact:

$$S_{\mu,\nu} \begin{cases} > 0 & \Rightarrow & \text{bonding} \\ = 0 & \Rightarrow & \text{nonbonding} \\ < 0 & \Rightarrow & \text{antibonding} \end{cases} \quad (2.9)$$

This is adequate to describe the simple AO/MO correlation diagrams found in first-year University chemistry courses (e.g., Fig. 2.1.)

**Dirac-Roothaan Representation** Sometimes it is useful to use a more compact representation. This is made possible using Dirac’s bras and kets. The bras and kets are related to the wavefunctions by,

$$\begin{aligned} \psi(\vec{r}) &= \langle \vec{r} | \psi \rangle \\ \phi^*(\vec{r}) &= \langle \phi | \vec{r} \rangle . \end{aligned} \quad (2.10)$$

Then,

$$\begin{aligned}
 \langle \phi | \psi \rangle &= \int \phi^*(\vec{r}) \psi(\vec{r}) d\vec{r} \\
 &= \int \langle \phi | \vec{r} \rangle \langle \vec{r} | \psi \rangle d\vec{r} \\
 &= \langle \phi | \left( \int |\vec{r}\rangle \langle \vec{r}| d\vec{r} \right) | \psi \rangle.
 \end{aligned} \tag{2.11}$$

Note how this implies the completeness relation,

$$\hat{1} = \int |\vec{r}\rangle \langle \vec{r}| d\vec{r}. \tag{2.12}$$

In bra-ket notation, Eq. (2.7) is written as,

$$|\psi_i\rangle = \sum_{\mu} |\chi_{\mu}\rangle C_{\mu,i}, \tag{2.13}$$

or,

$$\vec{\psi}^{\dagger} = \vec{\chi}^{\dagger} \mathbf{C}, \tag{2.14}$$

where,

$$\begin{aligned}
 \vec{\psi}^{\dagger} &= ( |\psi_1\rangle \quad |\psi_2\rangle \quad \cdots \quad |\psi_n\rangle ) \\
 \vec{\chi}^{\dagger} &= ( |\chi_1\rangle \quad |\chi_2\rangle \quad \cdots \quad |\chi_m\rangle ) \\
 \mathbf{C} &= \begin{bmatrix} C_{1,1} & C_{1,2} & \cdots & C_{1,n} \\ C_{2,1} & C_{2,2} & \cdots & C_{2,n} \\ \vdots & \vdots & \ddots & \vdots \\ C_{m,1} & C_{m,2} & \cdots & C_{m,n} \end{bmatrix}.
 \end{aligned} \tag{2.15}$$

Similarly,

$$\begin{aligned}
 \vec{\phi} &= \begin{pmatrix} \langle \psi_1 | \\ \langle \psi_2 | \\ \vdots \\ \langle \psi_n | \end{pmatrix} \\
 \vec{\chi} &= \begin{pmatrix} \langle \chi_1 | \\ \langle \chi_2 | \\ \vdots \\ \langle \chi_m | \end{pmatrix}.
 \end{aligned} \tag{2.16}$$

I call this combination of Dirac notation and matrix notation “Dirac-Roothaan notation” because the first time I saw it was in an article by Roothaan. This allows us to write some things very compactly:

$$\begin{aligned}
 \mathbf{S} = \vec{\chi} \vec{\chi}^{\dagger} &\Rightarrow \text{Overlap matrix} \\
 \mathbf{H} = \vec{\chi}^{\dagger} \hat{h} \vec{\chi} &\Rightarrow \text{Orbital Hamiltonian matrix} \\
 \hat{P} = \vec{\chi}^{\dagger} \mathbf{S}^{-1} \vec{\chi} &\Rightarrow \text{Resolution-of-the-identity}.
 \end{aligned} \tag{2.17}$$



Note that the resolution-of-the-identity (RI) only gives the identity operator,  $\hat{1}$ , in the limit of a complete basis set. Nevertheless, *assuming* that the RI projector is the identity operator provides a quick way to find the matrix form of the orbital equation that can be found more rigorously from the variational principle. This equation is solved in DEMON2K and other quantum chemistry programs:

$$\begin{aligned}\hat{h}|\psi_i\rangle &= \epsilon_i|\psi_i\rangle \\ \vec{\chi}\hat{h}\vec{P}|\psi_i\rangle &= \epsilon_i\vec{\chi}|\psi_i\rangle \\ \vec{\chi}\hat{h}\vec{\chi}^\dagger\mathbf{S}^{-1}\vec{\chi}|\psi_i\rangle &= \epsilon_i\vec{\chi}|\psi_i\rangle \\ \mathbf{H}\vec{C}_i &= \epsilon_i\mathbf{S}\vec{C}_i,\end{aligned}\tag{2.18}$$

where,

$$\vec{C}_i = \mathbf{S}^{-1}\vec{\chi}|\psi_i\rangle,\tag{2.19}$$

is the  $i$ th column of the matrix  $\mathbf{C}$  of MO coefficients because,

$$\begin{aligned}|\psi_i\rangle &= \vec{\chi}^\dagger\vec{C}_i \\ \vec{\chi}|\psi_i\rangle &= \vec{\chi}\vec{\chi}^\dagger\vec{C}_i \\ \vec{\chi}|\psi_i\rangle &= \mathbf{S}\vec{C}_i \\ \vec{C}_i &= \mathbf{S}^{-1}\vec{\chi}|\psi_i\rangle.\end{aligned}\tag{2.20}$$

One nice thing about the Dirac-Roothaan representation is that it provides useful tools for dealing with basis sets which are *not* orthonormal, which is almost always the case in quantum chemistry.

It is worth repeating that the matrix form of the orbital equation solved in most quantum chemistry program is,

$$\mathbf{H}\vec{C}_i = \epsilon_i\mathbf{S}\vec{C}_i,\tag{2.21}$$

which is a sort of generalized eigenvalue problem. It is often solved using Lödwin's method which involves taking the square root of the overlap matrix:

$$\begin{aligned}\mathbf{H}\mathbf{S}^{-1/2}\mathbf{S}^{+1/2}\vec{C}_i &= \epsilon_i\mathbf{S}^{+1/2}\mathbf{S}^{+1/2}\vec{C}_i \\ (\mathbf{S}^{-1/2}\mathbf{H}\mathbf{S}^{-1/2})\left(\mathbf{S}^{+1/2}\vec{C}_i\right) &= \epsilon_i\left(\mathbf{S}^{+1/2}\vec{C}_i\right) \\ \tilde{\mathbf{H}}\tilde{C}_i &= \epsilon_i\tilde{C}_i,\end{aligned}\tag{2.22}$$

where objects indicated with a tilde are sometimes called the symmetrized quantities,

$$\begin{aligned}\tilde{\mathbf{H}} &= \mathbf{S}^{-1/2}\mathbf{H}\mathbf{S}^{-1/2} \\ \tilde{C}_i &= \mathbf{S}^{+1/2}\vec{C}_i.\end{aligned}\tag{2.23}$$

A final calculation is then needed to retrieve the true MO coefficients,

$$\vec{C}_i = \mathbf{S}^{-1/2}\tilde{C}_i.\tag{2.24}$$

**Gaussian-type Orbitals** The LCAO approximation is only a starting point for accurate approximations which use more elaborate basis sets. There are many excellent reviews of the basis sets used in quantum chemistry (e.g., Ref. [36, 37]). These should be studied. My goal here is only to give a minimal overview.

Although some programs (e.g., DMOL [38]) actually start with real atomic orbitals obtained from atomic calculations on many-electron atoms, most programs take a different approach.

True AOs look roughly like hydrogen atom orbitals which take the familiar form,

$$\chi_{n,l,m}(\vec{r}) = Y_{l,m}(\theta, \phi) R_{n,l}(r), \quad (2.25)$$

where the radial function is a polynomial times an exponential. For example,

$$\begin{aligned} R_{1s}(r) &= 2 \left( \frac{Z}{a_0} \right)^{3/2} e^{-Zr/a_0} \\ R_{2s}(r) &= \frac{1}{\sqrt{2}} \left( \frac{Z}{a_0} \right)^{3/2} \left( 1 - \frac{Zr}{2a_0} \right) e^{-Zr/a_0} \\ R_{2p}(r) &= \frac{1}{2\sqrt{6}} \left( \frac{Z}{a_0} \right)^{5/2} r e^{-Zr/a_0}, \end{aligned} \quad (2.26)$$

where  $a_0$  is the Bohr radius and  $Z$  is the atomic number of the 1-electron atom. As the nodes in the radial wave function are due to the requirement that the higher energy orbitals be orthogonal to the lower energy orbitals and as this orthogonalization emerges naturally in variational calculations, it is enough to use Slater-type orbitals (STOs) of the form, STO

$$\chi_{n,l,m}(\vec{r}) \propto Y_{l,m}(\theta, \phi) r^{n-1} e^{-\zeta r/a_0}. \quad (2.27)$$

In many-electron atoms, the real atomic number  $Z$  is replaced by an effective atomic number  $\zeta$  (Greek letter *zeta*) which may, for example, be determined by Slater's rules [39]. The problem with spherical-harmonic STOs in the form of Eq. (2.27) is that these STOs are complex valued which is a problem both for visualization and because it increases computation times. However spherical-harmonic orbitals may be made the real and imaginary parts if necessary,

$$\begin{aligned} Y_{0,0} &= \frac{1}{2\sqrt{\pi}} \\ Y_{1,0} &= \frac{1}{2} \sqrt{\frac{3}{\pi}} \frac{z}{r} \\ \Re Y_{1,1} &= \frac{1}{2} \sqrt{\frac{3}{2\pi}} \frac{x}{r} \\ \Im Y_{1,1} &= \frac{1}{2} \sqrt{\frac{3}{2\pi}} \frac{y}{r}. \end{aligned} \quad (2.28)$$

This allows the spherical STOs to be replaced by cartesian STOs of the form,

$$\chi_{l_x, l_y, l_z}(\vec{r}) \propto x^{l_x} y^{l_y} z^{l_z} e^{-\zeta r/a_0}. \quad (2.29)$$

Here  $l = l_x + l_y + l_z$  is more or less the azimuthal quantum number except that certain combinations actually lead to functions of lower azimuthal quantum number. For example, there is no  $d_{x^2+y^2+z^2}$  function because  $x^2 + y^2 + z^2 = r^2$  is spherically symmetric, hence an  $s$  function. STOs are used in some programs, such as ADF [40], electron repulsion integrals involving more than two centers are difficult to evaluate using STOs. ADF

Instead it is better to use Gaussian-type orbitals (GTOs) of either the spherical-harmonic or cartesian type. These differ from STOs by the replacement  $\exp(-\zeta r/a_0)$  by  $\exp(-\alpha r^2/a_0^2)$  to make primitive GTOs, GTO

$$\chi_{l_x, l_y, l_z}(\vec{r}; \alpha) \propto x^{l_x} y^{l_y} z^{l_z} e^{-\alpha r^2/a_0^2}. \quad (2.30)$$

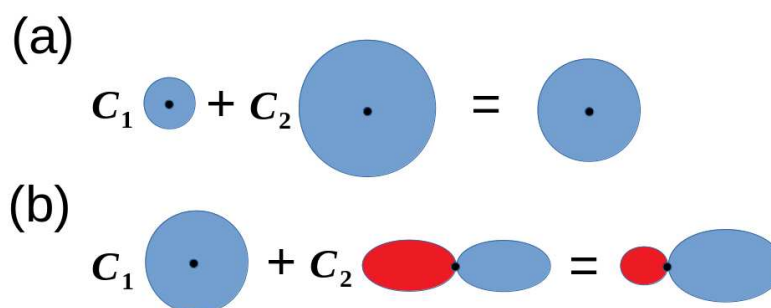


Figure 2.2: Illustration of the effects of using (a) a double  $\zeta$  basis set and (b) a polarization function.

Fixed linear combinations of primitive GTOs make contracted GTOs of the form,

$$\chi_\mu(\vec{r}) \propto x^{l_x} y^{l_y} z^{l_z} \sum_i e^{-\alpha_i r^2 / a_0^2} d_i. \quad (2.31)$$

Here the  $d_i$  are the contraction coefficients and the  $\alpha_i$  are the exponentials. DEMON2K uses a GTO basis set.

Contracted GTOs may resemble STOs as in the case of the STO-3G basis minimal basis set where each STO is approximated by a linear combination of three primitive GTOs. Note that a *minimal basis set* corresponds to the case where there is one orbital for each core and for each valence orbital (whether the latter are occupied or not). This partly justifies the common practice of referring to GTOs as AOs.

One criticism which is sometimes made of GTOs by physicists who are used to planewave codes is that there is no single parameter (like the wave number cut-off) that can be used to control the convergence of the basis set. It is possible to control the convergence of a GTO basis set in a systematic way by using, for example, even-tempered Gaussians which are known to provide a uniform coverage of the function space and by systematically enlarging the angular degree of freedom by increasing the largest azimuthal quantum number  $l$  in the basis set. However this is rarely done because chemists usually want the *smallest* basis set which is adequate for studying the molecular system (or systems) of interest to them. So the usual strategy is to expand the minimal basis set in two ways.

The first way is to double or triple (double  $\zeta$  or triple  $\zeta$ ) the number of AOs (i.e., really GTOs) so as to allow expansion or contraction of the AO by variational optimization of, for example, a linear combination of a smaller and a larger GTO of the same type (Fig. 2.2a.) The second way is to include polarization functions of higher angular momentum than in the minimal basis which may be used to describe an angular deformation of an atom or polarization of a bond (Fig. 2.2b.) Clearly these tight or diffuse or polarization functions are no longer atomic orbitals, but it is still common practice to call them AOs.

A convenient place to find GTO basis sets is at the **Basis Set Exchange**:

<https://www.basissetexchange.org/>. You can even download GTO basis sets specifically in DEMON2K format!

**BASIS file** The DEMON2K BASIS file is a library of orbital basis sets. For example, for the hydrogen atoms, the file includes the following orbital basis sets:

1. O-HYDROGEN HYDROGEN H (41) (DZV) (DZV-LDA)

2. O-HYDROGEN HYDROGEN H (41/1) (DZVP) (DZVP-LDA) [41]
3. O-HYDROGEN HYDROGEN H (DZV-GGA)
4. O-HYDROGEN HYDROGEN H (DZVP-GGA) [42]
5. O-HYDROGEN HYDROGEN H (41/11\*) (TZVP)
6. O-HYDROGEN HYDROGEN H (3) (STO-3G) [43]
7. O-HYDROGEN HYDROGEN H (6-31G\*\*) [44, 45]
8. O-HYDROGEN HYDROGEN H (6-311G\*\*) [46]
9. O-HYDROGEN HYDROGEN H (DEF2-TZVPP) [47]
10. O-HYDROGEN HYDROGEN H (3111/11) (EPR) (EPR-III) [48]
11. O-HYDROGEN HYDROGEN H (311/1) (IGLO-II) [49]
12. O-HYDROGEN HYDROGEN H (3111/11) (IGLO-III) [49]
13. O-HYDROGEN HYDROGEN H (LIC) [50]
14. O-HYDROGEN HYDROGEN H (SAD) [51]
15. O-HYDROGEN HYDROGEN H (41/1\*) (TZVP-FIP1) [52]
16. O-HYDROGEN HYDROGEN H (41/1\*/1+) (TZVP-FIP2) [52]
17. O-HYDROGEN HYDROGEN H (DZ-ANO) [53]
18. O-HYDROGEN HYDROGEN H (cc-pVTZ) [54]
19. O-HYDROGEN HYDROGEN H (AUG-CC-PVDZ) [55]
20. O-HYDROGEN HYDROGEN H (AUG-CC-PVTZ) [55]
21. O-HYDROGEN HYDROGEN H (AUG-CC-PVQZ) [55]
22. O-HYDROGEN HYDROGEN H (AUG-CC-PV5Z) [55]
23. O-HYDROGEN H (AUG-PCJ-0) [56]
24. O-HYDROGEN H (AUG-PCJ-1) [56]
25. O-HYDROGEN H (AUG-PCJ-2) [56]
26. O-HYDROGEN H (AUG-PCJ-3) [56]
27. O-HYDROGEN H (AUG-PCJ-4) [56]
28. O-HYDROGEN HYDROGEN H (LANL2DZ) [57]

It is also possible to input your own basis set (possibly one downloaded from the **Basis Set Exchange**) via the standard DEMON2K input file.

Let us take a look at the format of one of these basis sets to get an idea of what the numbers mean:

```
O-HYDROGEN HYDROGEN H (SAD)
5
1 0 4
    33.8650140000      0.0060680000
    5.0947880000      0.0453160000
    1.1587860000      0.2028460000
    0.3258400000      0.5037090000
2 0 1
    0.1027410000      1.0000000000
3 0 1
    0.0324000000      1.0000000000
2 1 2
    1.1588000000      0.1884400000
    0.3258000000      0.8824200000
3 1 2
    0.1027000000      0.1178000000
    0.0324000000      0.0042000000
```

This is an example of a Sadlej field-induced polarisation basis which is specifically designed for efficient calculation of molecular polarizabilities. The number “5” after the title tells us that this basis set consists of 5 contracted GTOs. The next line “1 0 4” tells us the following lines describe the first (“1”)  $s$ -type ( $l = 0$ ) function which is a contraction of 4 primitive GTOs. The exponents and contraction coefficients are:

1s

1.  $\alpha_1 = 33.8650140000$ ,  $d_1 = 0.0060680000$
2.  $\alpha_2 = 5.0947880000$ ,  $d_2 = 0.0453160000$
3.  $\alpha_3 = 1.1587860000$ ,  $d_3 = 0.2028460000$
4.  $\alpha_4 = 0.3258400000$ ,  $d_4 = 0.5037090000$

The line “2 0 1” announces the next basis function which is the second  $s$ -type function consisting of a single primitive GTO:

1s'

1.  $\alpha_1 = 0.1027410000$ ,  $d_1 = 1.0000000000$

The line “3 0 1” announces the third basis function which is the third  $s$ -type function consisting of a single primitive GTO:

1s''

1.  $\alpha_1 = 0.0324000000$ ,  $d_1 = 1.0000000000$



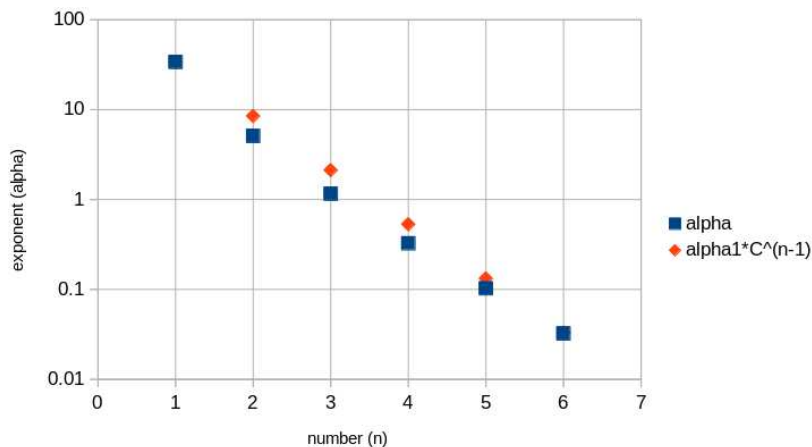


Figure 2.3: The exponents in the Sadlej basis set showing that they form a rough geometric series of the form  $\alpha_n = \alpha_1 * (C^{n-1})$  where  $C = 0.25$ .

Figure 2.3 shows how the exponents form a rough geometric series. This is not an accident but instead a property that has to be satisfied when GTOs provide a uniform coverage of function space [58]. Continuing on to the next lines: The line “2 1 2” announces the first set of  $p$ -type functions consisting of the contraction of two primitive GTOs:

$2p_x, 2p_y, 2p_z$

1.  $\alpha_1 = 1.1588000000, d_1 = 0.1884400000$

2.  $\alpha_2 = 0.3258000000, d_2 = 0.8824200000$

This is followed by the line “3 1 2” which announces the second set of  $p$ -type functions which also consists of the contraction of two primitive GTOs:

$2p'_x, 2p'_y, 2p'_z$

1.  $\alpha_1 = 0.1027000000, d_1 = 0.1178000000$

2.  $\alpha_2 = 0.0324000000, d_2 = 0.0042000000$

The total size of the basis set is  $m = 3$   $s$ -type functions + 2 sets of 3  $p$ -type functions = 9 AOs.

### 2.3.3 Dissociation Energy

The ground-state bond energy or dissociation energy  $D_e$  of  $H_2$  is,

$D_e, D_0$

$$D_e = 2E(H) - E(H_2). \quad (2.32)$$

(When the zero-point vibrational energy is included, this quantity is known as  $D_0$ .) For some of the excited states, the dissociation energy is,

$$D_e = (E(H^+) + E(H^-)) - E(H_2). \quad (2.33)$$

It is clear that you must calculate the following energies:  $H^+$ ,  $H$ ,  $H^-$ , and  $H_2$  at its equilibrium geometry. I recommend that you use a spread sheet (such as EXCEL or LIBREOFFICE CALC) to keep track of these energies. We will use the Sadlej basis set and many program defaults. *The first energies to calculate are the atomic energies.*

**H<sup>+</sup>** Copy the following input file and run DEMON2K:

```
TITLE H+ (Basis: SAD/GEN-A3*)
CHARGE +1
MULTI 1
#
SCFTYPE UKS
VXCTYPE VWN
#
PRINT MOS
#
# --- GEOMETRY ---
#
#
GEOMETRY CARTESIAN BOHR
H      0.000000      0.000000      0.000000
#
AUXIS (GEN-A3*)
BASIS (SAD)
```

Note down:

1. The size of the basis set (number of AOs)
2. The total energy in Ha (hartrees)
3. The spin  $\alpha$  and spin  $\beta$  orbital energies
4. Anything else you find interesting.

Discuss your results.

**H** Copy the following input file and run DEMON2K:

```
TITLE H (Basis: SAD/GEN-A3*)
CHARGE 0
MULTI 2
#
SCFTYPE UKS
VXCTYPE VWN
#
PRINT MOS
#
# --- GEOMETRY ---
#
#
GEOMETRY CARTESIAN BOHR
H      0.000000      0.000000      0.000000
H      0.000000      0.000000      5.000000
#
```

AUXIS (GEN-A3\*)  
BASIS (SAD)

Note down:

1. The size of the basis set (number of AOs)
2. The total energy in Ha (hartrees)
3. The spin  $\alpha$  and spin  $\beta$  orbital energies
4. Anything else you find interesting.

Discuss your results.

**H<sup>-</sup>** Copy the following input file and run DEMON2K:

```
TITLE H- (Basis: SAD/GEN-A3*)
CHARGE -1
MULTI 1
#
SCFTYPE UKS
VXCTYPE VWN
#
PRINT MOS
#
# --- GEOMETRY ---
#
#
GEOMETRY CARTESIAN BOHR
H      0.000000    0.000000    0.000000
#
AUXIS (GEN-A3*)
BASIS (SAD)
```

Note down:

1. The size of the basis set (number of AOs)
2. The total energy in Ha (hartrees)
3. The spin  $\alpha$  and spin  $\beta$  orbital energies
4. Anything else you find interesting.

Discuss your results.

**H<sub>2</sub>** Obtaining the equilibrium energy of H<sub>2</sub> requires a geometry optimization. Copy the following input file and run DEMON2K:

```
TITLE H2 (Basis: SAD/GEN-A3*)
CHARGE -1
MULTI 1
#
SCFTYPE UKS
OPTIMIZATION
VXCTYPE VWN
#
PRINT MOS
#
# --- GEOMETRY ---
#
#
GEOMETRY CARTESIAN BOHR
H      0.000000    0.000000    0.000000
#
AUXIS (GEN-A3*)
BASIS (SAD)
```

Note down:

1. Check that the calculations are correctly converged.
2. Determine the equilibrium bond length and total energy.
3. Determine the bond dissociation energy.
4. From an examination of the MO coefficients, sketch cartoons of the first 9 MOs at the equilibrium geometry.
5. Anything else you find interesting.

Discuss your results.

### 2.3.4 Excited States

There are various ways to treat excited states in DFT. We will examine a few of these here and then try to calculate the vertical excitation energies for a few states using a couple of different methods.

**Textbook MO Model** Every first-year University-level General Chemistry course discusses MO theory for at least a few homonuclear diatomic molecules, the first of which is typically H<sub>2</sub>. Let us label the atoms: H<sub>A</sub>-H<sub>B</sub>. The atom is fixed in space and is traditionally oriented along the *z*-axis. Just as when studying crystals, symmetry is very important when studying small molecules in order to understand selection rules governing which orbitals are zero and which are nonzero. The H<sub>2</sub> molecule has axial symmetry (rotation around the *z*-axis leaves the molecule unchanged), has mirror symmetry [reflection around the (*x*, *y*) mirror plane (*plan miroir* in French) bisecting the H-H axis leaves the molecule unchanged], and there is also a center of inversion symmetry in the middle of the

bond. We will take the usual minimal basis of a single  $1s$  orbital on each atom. The  $1s$  AO on  $H_A$  will be referred to as  $s_A$  and the  $1s$  AO on  $H_B$  will be referred to as  $s_B$ . According to group theory, the MOs must belong to irreducible representations (irreps) of the molecule. In the first instance, we will only be concerned with orbitals with cylindrical symmetry with respect to rotation around the bond axis (i.e.,  $\sigma$  orbitals) and even or odd symmetry with respect to reflection through the center of inversion (same, in the present simple model, as reflection through the mirror plane). We may make two MOs—namely,

irrep

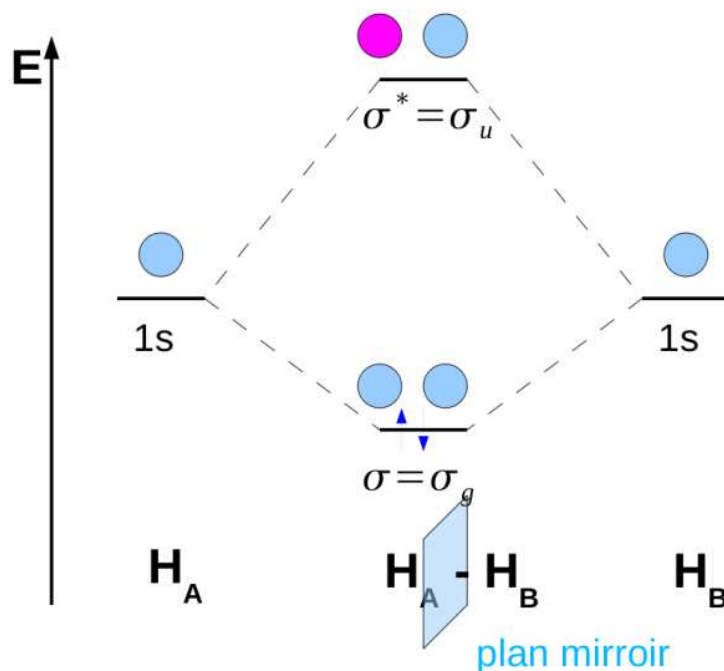
$$\begin{aligned}\sigma_g &= \frac{1}{\sqrt{2(1+S)}}(s_A + s_B) \\ \sigma_u &= \frac{1}{\sqrt{2(1-S)}}(s_A - s_B),\end{aligned}\quad (2.34)$$

where,

$$S = \langle s_A | s_B \rangle = \langle s_B | s_A \rangle, \quad (2.35)$$

is the overlap matrix. As written, the two MOs are orthonormal. They are used to construct the orbital correlation diagram (OCD):

overlap  
matrix  
OCD



Notice that the MOs are always represented using lower case letters.

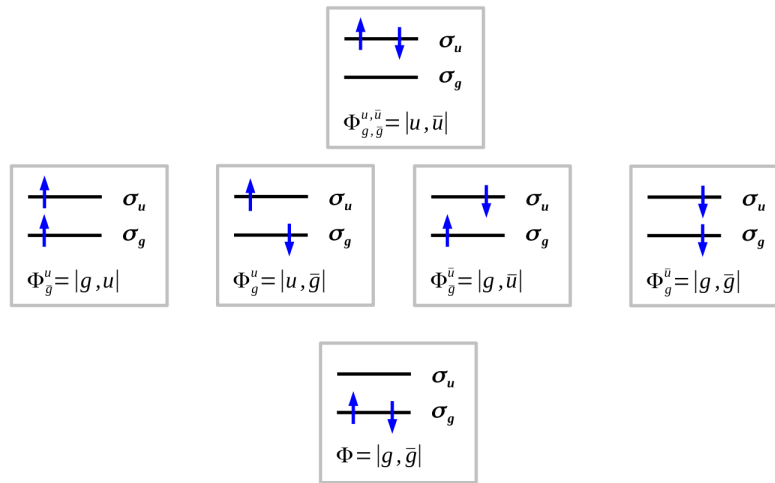
*A long-standing tradition requires that, whenever possible, lower case Greek and Latin letters be used for orbital quantities, while upper case Greek and Latin letters are reserved for many-electron (state) quantities.*

The subscript  $g$  stands for *gerade* (even in German) while  $u$  states for *ungerade* (odd in German). The MO names  $\sigma_u$  and  $\sigma_g$  emphasize the symmetry. Most General Chemistry textbooks use  $\sigma$  for the bonding MO and  $\sigma^*$  for the antibonding MO. We prefer the symmetry notation.

TOTEM

We now have a two-orbital two-electron model (TOTEM) problem from which we wish to construct wave functions. The TOTEM is a  $(2/2)$  model where  $(n/m)$  refers to  $n$  electrons in  $m$  orbitals. There are several ways to occupy MOs in our TOTEM:





The state energies have been ordered using a zero-order estimate neglecting electron repulsions so that the energy is just given by the total of the orbital energies. Thus the lowest energy orbital is doubly occupied in the ground state and the highest energy orbital is doubly occupied in the highest energy excited state. In-between, we have four states which are energetically degenerate in the zero-order approximation. This is the famous *spin multiplet problem*. This is a common feature in molecular spectroscopy and photochemistry but is rarely studied in solid-state physics because of the complexity of spin-coupling Avogadro's number of electrons. Nevertheless it does come up in solid-state physics in the Kondo effect and in Josephson junctions. A full explanation of spin-coupling is quite complicated [15] and would take us too far away from our objectives. Fortunately, we will show that the situation is much easier when we only have two electrons because the 2-electron wave function factors into a space and a spin part. As the entire wave function must be antisymmetric, one but not both of the two factors into which the wave function separates must be antisymmetric while the other is symmetric. Let us see exactly how this happens.

spin mul-  
tiplet

Note that I use a short-hand notation for a Slater determinant, namely

$$\begin{aligned}
 |r, s| &= \frac{1}{\sqrt{2}} \begin{vmatrix} \phi_r(1) & \phi_s(1) \\ \phi_r(2) & \phi_s(2) \end{vmatrix} \\
 &= \frac{1}{\sqrt{2}} (\phi_r(1)\phi_s(2) - \phi_s(1)\phi_r(2)) ,
 \end{aligned} \tag{2.36}$$

where  $i$  stands for the coordinates of electron  $i$ . In addition  $\bar{i}$  stands for the spatial orbital  $i$  times the  $\beta$  ( $\downarrow$ ) spin function while  $i$  stands for the same thing except times the  $\alpha$  ( $\uparrow$ ) spin function. Therefore

$$\begin{aligned}
 |g, \bar{g}| &= \frac{1}{\sqrt{2}} (g(1)\alpha(1)g(2)\beta(2) - g(1)\beta(1)g(2)\alpha(2)) \\
 &= (\sigma_g(1)\sigma_g(2)) \left[ \frac{1}{\sqrt{2}} (\alpha(1)\beta(2) - \beta(1)\alpha(2)) \right] .
 \end{aligned} \tag{2.37}$$

(I am using  $g$  as synonymous with  $\sigma_g$  and similarly for  $u$ .)  $|g, \bar{g}|$  is a  $\Sigma_g$  wave function because it is cylindrically symmetric around the bond axis and because it is even with respect to inversion symmetry. Similarly,

$$\begin{aligned}
 |u, \bar{u}| &= \frac{1}{\sqrt{2}} (u(1)\alpha(1)u(2)\beta(2) - u(1)\beta(1)u(2)\alpha(2)) \\
 &= (\sigma_u(1)\sigma_u(2)) \left[ \frac{1}{\sqrt{2}} (\alpha(1)\beta(2) - \beta(1)\alpha(2)) \right] ,
 \end{aligned} \tag{2.38}$$

is also  $\Sigma_g$  (because odd  $\times$  odd = even).

Now let us turn specifically to the spin multiplet states! Since,

$$\begin{aligned} |g, u| &= \frac{1}{\sqrt{2}} (g(1)\alpha(1)u(2)\alpha(2) - u(1)\alpha(1)g(2)\alpha(2)) \\ &= \left[ \frac{1}{\sqrt{2}} (\sigma_g(1)\sigma_u(2) - \sigma_u(1)\sigma_g(2)) \right] (\alpha(1)\alpha(2)) , \end{aligned} \quad (2.39)$$

then we have a  $\Sigma_u$  state. Also

$$\begin{aligned} |\bar{g}, \bar{u}| &= \frac{1}{\sqrt{2}} (g(1)\beta(1)u(2)\beta(2) - u(1)\beta(1)g(2)\beta(2)) \\ &= \left[ \frac{1}{\sqrt{2}} (\sigma_g(1)\sigma_u(2) - \sigma_u(1)\sigma_g(2)) \right] (\beta(1)\beta(2)) , \end{aligned} \quad (2.40)$$

is a  $\Sigma_u$  state. However, neither  $|u, \bar{g}|$  nor  $|g, \bar{u}|$  factor into the product of a spatial part and a spin part. Ultimately this is because they are not eigenstates of the  $\hat{S}^2$  operator, though they are eigenstates of  $\hat{S}_z$  with eigenvalue,

$$M_S = \frac{n_\alpha - n_\beta}{2} , \quad (2.41)$$

which is zero for  $\Phi_M = |u, \bar{g}|$  and for  $\Phi_{\bar{M}} = |g, \bar{u}|$ . Often we call them symmetry-mixed states or just mixed states. We can use them to create eigenstates of  $\hat{S}^2$  by taking the normalized  $\pm$  combinations:

mixed  
states

$$\begin{aligned} \frac{1}{\sqrt{2}} (|u, \bar{g}| \pm |g, \bar{u}|) &= \frac{1}{2} (u(1)\alpha(1)g(2)\beta(2) - g(1)\beta(1)u(2)\alpha(2)) \pm \frac{1}{2} (g(1)\alpha(1)u(2)\beta(2) - u(1)\beta(1)g(2)\alpha(2)) \\ &= \left[ \frac{1}{\sqrt{2}} (u(1)g(2) \pm g(1)u(2)) \right] \left[ \frac{1}{\sqrt{2}} (\alpha(1)\beta(2) \mp \beta(1)\alpha(2)) \right] . \end{aligned} \quad (2.42)$$

These are  $\Sigma_u$  states as well.

We now make use of the fact that we are neglecting all spin-orbit terms in our (electronic) hamiltonian,

$$\begin{aligned} \hat{H} &= \hat{h}(1) + \hat{h}(2) + \frac{1}{r_{1,2}} - \frac{1}{|\vec{r}_1 - \vec{R}_A|} \\ \hat{h} &= -\frac{1}{2}\nabla^2 - \frac{1}{|\vec{r} - \vec{R}_A|} - \frac{1}{|\vec{r} - \vec{R}_B|} . \end{aligned} \quad (2.43)$$

Then a wave function  $\Psi = \Psi_{\text{space}}\Psi_{\text{spin}}$  that factors into a space and a spin part has an energy which is independent of the spin part and so depends only on the space part,

$$E = \langle \Psi | \hat{H} | \Psi \rangle = \langle \Psi_{\text{space}} | \hat{H} | \Psi_{\text{space}} \rangle . \quad (2.44)$$

Consequently, our multiplet spin problem resolves into a non-degenerate open-shell *singlet state*,

singlet  
state

$$\begin{aligned} \Psi_{0,0} &= \frac{1}{\sqrt{2}} (|u, \bar{g}| + |g, \bar{u}|) \\ \Psi_{\text{space}}^{\text{singlet}} &= \frac{1}{\sqrt{2}} (\sigma_g(1)\sigma_u(2) + \sigma_u(1)\sigma_g(2)) , \end{aligned} \quad (2.45)$$

and three energetically-degenerate triplet states,

vertical  
state

$$\begin{aligned}
 \Psi_{1,+1} &= |g, u| \\
 \Psi_{1,0} &= \frac{1}{\sqrt{2}} (|g, \bar{u}| - |u, \bar{g}|) \\
 \Psi_{1,-1} &= |\bar{g}, \bar{u}| \\
 \Psi_{\text{space}}^{\text{triplet}} &= \frac{1}{\sqrt{2}} (\sigma_g(1)\sigma_u(2) - \sigma_u(1)\sigma_g(2)) ,
 \end{aligned} \tag{2.46}$$

Here I have introduced the notation  $\Psi_{S,M_S}$  where  $S$  and  $M_S$  are spin quantum numbers,

$$\begin{aligned}
 \hat{S}^2 \Psi_{S,M_S} &= S(S+1) \Psi_{S,M_S} \\
 \hat{S}_z \Psi_{S,M_S} &= M_S \Psi_{S,M_S} .
 \end{aligned} \tag{2.47}$$

**Ziegler-Rauk-Baerends Multiplet Sum Model** For all practical purposes, DFT is a SDET theory. However it is quite clear that the spin multiplets involve MDET wave functions. What to do? Ziegler, Rauk, and Baerends gave a clear answer pratical answer with their multiplet sum model (MSM) [59].

MSM

To be clear, this is not a formally justified method but rather a practical approach based upon reasonable physical intuition. Exact DFT applies only to (non-interacting  $v$ -representable) ground states and certainly not to excited states. Nevertheless it is common practice to assume that DFT may be used for the lowest state of each symmetry. This is really based upon the idea that all of the common density-functional approximations (DFAs) do a good job of describing *dynamical correlation* which is the residual electron correlation when a SDET wave function is a good first approximation. This is certainly the case for the  $\Psi_{1,+1} = |g, u|$  state! Hence we may use this state in DFT to calculate the lowest triplet energy. But what about the corresponding open-shell singlet  $\Psi_{0,0}$ ? For this, we need to use symmetry arguments to remove the zeroeth order degeneracy of our states. Correlation due to degeneracies (and hence associated with symmetry) is called *static correlation*. The MSM is based upon the observation that the singlet and triplet energies may be written as,

DFA, dynamical correlation

static correlation

$$\begin{aligned}
 E_T &= \langle g, u | \hat{H} | g, u \rangle = E[g, u] \\
 E_T &= \frac{1}{2} (\langle g, \bar{u} | - \langle u, \bar{g} |) \hat{H} | g, \bar{u} \rangle - |u, \bar{g} \rangle) \\
 &= \langle g, \bar{u} | \hat{H} | g, \bar{u} \rangle - \langle g, \bar{u} | \hat{H} | u, \bar{g} \rangle \\
 E_S &= \frac{1}{2} (\langle g, \bar{u} | - \langle u, \bar{g} |) \hat{H} | g, \bar{u} \rangle + |u, \bar{g} \rangle) \\
 &= \langle g, \bar{u} | \hat{H} | g, \bar{u} \rangle + \langle g, \bar{u} | \hat{H} | u, \bar{g} \rangle .
 \end{aligned} \tag{2.48}$$

Hence, *assuming that the MOs used to construct the two states are the same*, we may calculate the triplet and open-shell singlet energies using only SDET energies,

$$\begin{aligned}
 E_S &= 2E_M - E_T \\
 E_T &= \langle g, u | \hat{H} | g, u \rangle = E[g, u] \\
 E_M &= \langle g, \bar{u} | \hat{H} | g, \bar{u} \rangle = E[g, \bar{u}] .
 \end{aligned} \tag{2.49}$$

## Time-Dependent Density-Functional Theory

# Chapter 3

## Answers

### 3.1 Answers for Section 2.3

#### 3.1.1 Bond Dissociation Energy

The Sadlej basis set for H consists of 3 *s*-type GTOs and 2 sets of *p*-type GTOs. As each set of *p*-type GTOs is composed of three functions ( $p_x$ ,  $p_y$ , and  $p_z$ ) then the total number of AOs in the Sadlej basis set consists of  $3 + 2 \times 3 = 9$  AOs. This is evident in the output files for the calculations of  $H^+$ , H, and  $H^-$ .

$H^+$  consists of a single positively charged nucleus and no electrons. Its energy is rigorously 0.0 Ha.

The Schrödinger equation for the H atom may be solved analytically and  $E(H) = -0.5$  Ha *exactly*. Of course, we do not get this with our finite basis sets and especially we do not get the exact answer because the LDA is not exact. Instead we get  $E(H) = -0.478497984$  Ha at the LDA/SAD/GEN-A3\* level. The spin  $\alpha$  MO coefficients are:

				1	2	3	4	5
				-0.2687	0.0318	0.1010	0.1010	0.1010
				1.0000	0.0000	0.0000	0.0000	0.0000
1	1	H	1s	0.6570	-0.2594	0.0000	0.0000	0.0000
2	1	H	2s	0.3907	-0.6886	0.0000	0.0000	0.0000
3	1	H	3s	0.0477	1.4265	0.0000	0.0000	0.0000
4	1	H	2py	0.0000	-0.0000	0.0000	0.0120	0.0000
5	1	H	2pz	0.0000	-0.0000	0.0000	0.0000	0.0120
6	1	H	2px	0.0000	-0.0000	0.0120	0.0000	0.0000
7	1	H	3py	0.0000	-0.0000	0.0000	0.9925	0.0000
8	1	H	3pz	0.0000	-0.0000	0.0000	0.0000	0.9925
9	1	H	3px	0.0000	-0.0000	0.9925	0.0000	0.0000
				6	7	8	9	
				0.4346	0.7971	0.7971	0.7971	
				0.0000	0.0000	0.0000	0.0000	

1	1	H	1s	-1.3684	-0.0000	-0.0000	-0.0000
2	1	H	2s	2.1851	-0.0000	-0.0000	-0.0000
3	1	H	3s	-1.0715	-0.0000	-0.0000	-0.0000
4	1	H	2py	0.0000	1.2774	-0.0000	-0.0000
5	1	H	2pz	0.0000	-0.0000	-0.0000	1.2774
6	1	H	2px	0.0000	-0.0000	1.2774	-0.0000
7	1	H	3py	0.0000	-0.8043	-0.0000	-0.0000
8	1	H	3pz	0.0000	-0.0000	-0.0000	-0.8043
9	1	H	3px	0.0000	-0.0000	-0.8043	-0.0000

MO 1 is a nodeless 1s AO, MO 2 is a 2s AO with a radial node, MOs 3-5 are 2p AOs, MO 6 is a 3s AO with two radial nodes, MOs 7-9 are 3p AOs with one radial node. Note though that the unoccupied AOs are unlikely to be very exact. Notice also that the energy of the 1s AO is  $\epsilon_{1s} = -0.2689$  Ha, which is considerably larger than the exact  $E(\text{H}) = -0.5$  Ha. Underbinding of electrons is typical of DFT because the xc-potential goes to zero too quickly at large distance from the nucleus. The spin  $\beta$  MO coefficients are:

## BETA MO COEFFICIENTS OF CYCLE 6

				1	2	3	4	5
				-0.0998	0.0648	0.1441	0.1441	0.1441
				0.0000	0.0000	0.0000	0.0000	0.0000
1	1	H	1s	0.3904	-0.2370	0.0000	0.0000	0.0000
2	1	H	2s	0.4241	-1.0656	0.0000	0.0000	0.0000
3	1	H	3s	0.3355	1.4932	0.0000	0.0000	0.0000
4	1	H	2py	0.0000	-0.0000	0.0000	0.0000	-0.0638
5	1	H	2pz	0.0000	-0.0000	-0.0638	0.0000	0.0000
6	1	H	2px	0.0000	-0.0000	0.0000	-0.0638	0.0000
7	1	H	3py	0.0000	-0.0000	0.0000	0.0000	1.0385
8	1	H	3pz	0.0000	-0.0000	1.0385	0.0000	0.0000
9	1	H	3px	0.0000	-0.0000	0.0000	1.0385	0.0000
				6	7	8	9	
				0.5919	0.9529	0.9529	0.9529	
				0.0000	0.0000	0.0000	0.0000	
1	1	H	1s	-1.4707	-0.0000	-0.0000	-0.0000	
2	1	H	2s	2.0214	-0.0000	-0.0000	-0.0000	
3	1	H	3s	-0.9182	-0.0000	-0.0000	-0.0000	
4	1	H	2py	0.0000	-0.0000	1.2759	-0.0000	
5	1	H	2pz	0.0000	-0.0000	-0.0000	1.2759	
6	1	H	2px	0.0000	1.2759	-0.0000	-0.0000	
7	1	H	3py	0.0000	-0.0000	-0.7440	-0.0000	
8	1	H	3pz	0.0000	-0.0000	-0.0000	-0.7440	

9	1	H	3px	0.0000	-0.7440	-0.0000	-0.0000
---	---	---	-----	--------	---------	---------	---------

Corresponding  $\alpha$  and  $\beta$  MOs typically have different energies in spin-unrestricted calculations.

According to the Wikipedia entry for the “Hydrogen anion,” the electron affinity (EA) of the hydrogen atom is 0.027716 Ha. As

EA

$$E(\text{H}^-) = E(\text{H}) - \text{EA} = -0.527716 \text{ Ha} . \quad (3.1)$$

Hence we can calculate the LDA/SAD/GEN-A3\* energy. First makes sure that you find the CONVERGED keyword in the output file! In this case, the calculation has converged. The LDA/SAD/GEN-A3\* value is  $E(\text{H}^-) = -0.51106$  Ha. The spin  $\alpha$  and  $\beta$   $1s$  orbital energies are the same  $\epsilon_{1s} = 0.0655$  Ha. As this is a positive energy, the electron is not even bound. Strictly speaking, *such a calculation cannot be converged with respect to the quality of the orbital basis set and so should be discarded*. However this is just an exercise, so we shall keep it.

The EXACT bond length of  $\text{H}_2$  is  $R_e = 1.4$  bohr. The corresponding bond energy is  $D_e = 0.1740$  Ha. The optimization of  $\text{H}_2$  started out with a very bad guess for the  $\text{H}_2$  bond length. 18 self-consistent field (SCF) calculations had to be converged. Each time forces were calculated and the atoms were moved to minimize the energy until the gradient of the energy was considered small enough for a geometry optimization convergence. We see

SCF

```
*** CONVERGED BY GRADIENT AND DISPLACEMENT CRITERIA ***
*** AFTER 17 OPTIMIZATION CYCLES ***
```

```
RMSQ FORCE :    0.0000003  MAXIMUM :    0.0003000  CONVERGED :YES
MAX FORCE   :    0.0000003  MAXIMUM :    0.0004500  CONVERGED :YES
RMSQ DR     :    0.0002969  MAXIMUM :    0.0012000  CONVERGED :YES
MAX DR      :    0.0002969  MAXIMUM :    0.0018000  CONVERGED :YES
```

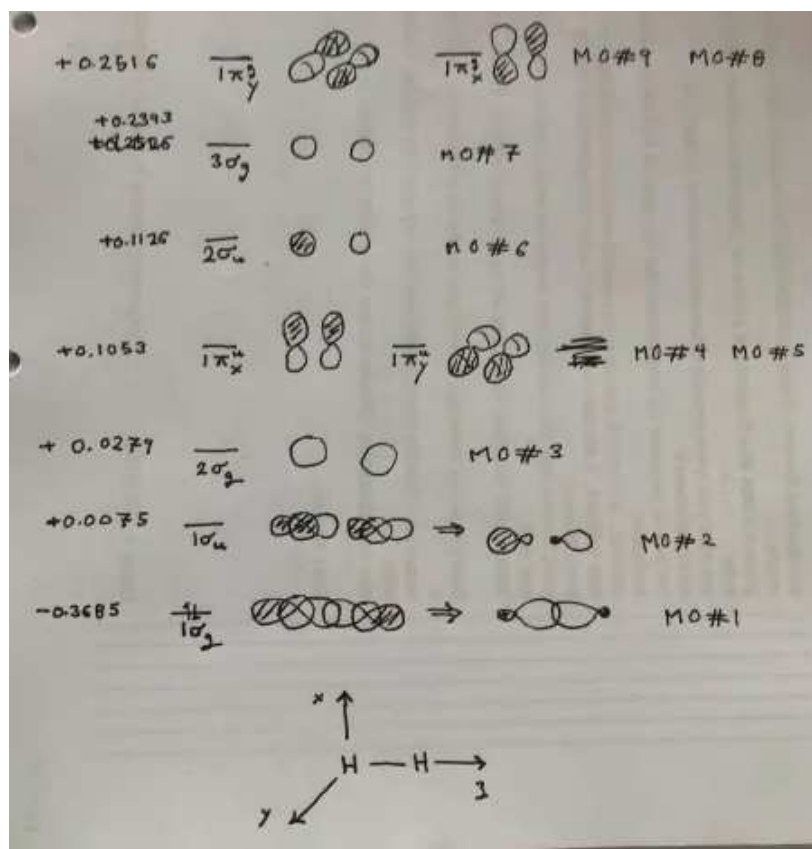
Our LDA/SAD/EN-A3\* calculations give

$$D_e = 2E(\text{H}) = E(\text{H}_2) = 2(-0.478497984 \text{ Ha}) - (-1.133460233 \text{ Ha}) = 0.1764642 \text{ Ha} . \quad (3.2)$$

The LDA is known to overbind molecules. In this case, the overbinding is by 0.025 Ha or 16 kcal/mol. This is much too large for accurate chemical calculations. The ideal chemical accuracy (i.e., the accuracy of thermodynamic bond energy measurements on small molecules) is 1 kcal/mol 0.001594 Ha.

chemical  
accuracy

Here are my sketches of the first nine MOs based upon their coefficients:



Note that software such as MOLDEN [60, 61, 62] may be used to visualize MOs produced by DE-MON2K. However it is a valuable learning step to be able to read MO coefficients and visualize from them what the MOs look like in the case of simple molecules.

MOLDEN

### 3.1.2 Excitation Energies



# Index

$D_0$ , 24  
 $D_e$ , 24  
APPLE, 11  
CENTOS, 11  
DMOL, 19  
LINUX, 11  
MOLDEN, 35  
UNIX, 11  
WINDOWS, 11  
DEMON2K, 3  
SHELL, 13  
AUXIS, 12  
BASIS, 12  
ECPS, 12  
FFDS, 12  
MCPS, 12  
binary, 12  
csh, 13  
deMon.inp, 13  
deMon.out, 13  
run.csh, 13  
  
AIP, 4  
AO, 5  
ASESMA, 3  
  
chemical accuracy, 34  
CI, 6  
  
DFA, 31  
DFT, 3  
dynamical correlation, 31  
  
EA, 34  
ELF, 5  
EXACT, 10  
  
GTO, 20  
  
Ha, 16  
  
HEG, 5  
  
irrep, 28  
  
jellium, 5  
  
LCAO, 6  
LDA, 8  
LDS, 5  
  
MDET, 4, 15  
mixed states, 30  
MO, 6  
MSM, 31  
  
OCD, 28  
overlap matrix, 28  
  
PC, 11  
PCCP, 4  
PEC, 4  
PES, 4  
  
Ry, 16  
  
SCF, 34  
SDET, 4  
SI, 15  
singlet state, 30  
spin multiplet, 29  
static correlation, 31  
STO, 20  
  
TD, 3  
TOTEM, 28  
triplet state, 30  
  
VB, 5  
VWN, 8  
  
xc, 12

# Bibliography

- [1] J. S. Rowlinson, [The border between physics and chemistry](#), Bull. Hist. Chem. **34**, 1 (2009).
- [2] G. N. Lewis, [The atom and the molecule](#), J. Am. Chem. Soc. **38**, 762 (1916).
- [3] W. B. Jensen, [A quantitative van Arkel diagram](#), J. Chem. Ed. **72**, 395 (1995).
- [4] C. S. McCaw and M. A. Thompson, [A new approach to chemistry education at pre-university level](#), Nature Chem. **1**, 95 (2009).
- [5] R. Rousseau and D. Marx, [Exploring the electronic structure of elemental lithium: From small molecules to nanoclusters, bulk metal, and surfaces](#), Chem. Eur. J. **6**, 2982 (2000).
- [6] E. Schrödinger, [An undulatory theory of the mechanics of atoms and molecules](#), Phys. Rev. **28**, 1049 (1926).
- [7] E. Schrödinger, [Quantisierung als Eigenwertproblem](#), Annalen der Physik **384**, 361 (1926).
- [8] W. Heitler and F. London, [Wechselwirkung neutraler Atome und homöopolare Bindung nach der Quantenmechanik](#), Zeitschrift für Physik **44**, 455 (1927).
- [9] L. Pauling, *The Nature of the Chemical Bond*, Cornell University Press, Ithaca, NY, USA, 3rd ed., 1960 edition, 1939.
- [10] G. W. Wheland, *The Theory of Resonance in Organic Chemistry and Its Application to Organic Chemistry*, Wiley, New York, 1955.
- [11] G. W. Wheland, *Resonance in Organic Chemistry*, Wiley, New York, 1955.
- [12] E. T. Strom, [George W. Wheland: Forgotten pioneer of resonance theory](#), in *Pioneers of Quantum Chemistry*, edited by E. T. Strom and A. K. Wilson, volume 1122, page 75, ACS Symposium Series, 2013.
- [13] G. W. Wheland, [The valence-bond treatment of the oxygen molecule](#), Trans. Faraday Soc. **33**, 1499 (1937).
- [14] P. A. M. Dirac, [Quantum mechanics of many-electron systems](#), Proc. Roy. Soc. A **123**, 714 (1929).
- [15] R. Pauncz, *Spin Eigenfunctions*, Plenum Press, New York, 1979.
- [16] C. A. Coulson and I. Fischer, [XXXIV. Notes on the molecular orbital treatment of the hydrogen molecule](#), Phil. Mag. **40**, 386 (1949).
- [17] D. L. Cooper, editor, volume 10 of *Theoretical and Computational Chemistry*, Elsevier, Amsterdam, 2002.

- [18] G. A. Gallup, *Valence Bond Methods: Theory and Applications*, Cambridge University Press, Cambridge, UK, 2002.
- [19] S. S. Shaik and P. C. Hiberty, *A Chemist's Guide to Valence Bond Theory*, John Wiley & Sons, Inc., Hoboken, New Jersey, USA, 2008.
- [20] T. E. Sharp, [Potential-energy curves for hydrogen and its ions](#), Atomic Data **2**, 119 (1971).
- [21] T. E. Sharp, [Erratum \[\*atomic data\* 2, 119 \(1971\)\]](#), Atomic Data **3**, 299 (1971).
- [22] S. H. Vosko, L. Wilk, and M. Nusair, [Accurate spin-dependent electron liquid correlation energies for local spin density calculations: a critical analysis](#), Can. J. Phys. **58**, 1200 (1980).
- [23] W. Kołos and L. Wolniewicz, [Potential energy curves for the  \$X\ ^1\Sigma\_g^+\$ ,  \$b\ ^3\Sigma\_u^+\$ , and  \$c\ ^1\pi\_u\$  states of the hydrogen molecule](#), J. Chem. Phys. **43**, 2429 (1965).
- [24] W. Kołos and L. Wolniewicz, [Potentialenergy curve for the  \$B\ ^1\Sigma\_u^+\$  state of the hydrogen molecule](#), J. Chem. Phys. **45**, 509 (1966).
- [25] W. Kołos and L. Wolniewicz, [Vibrational and rotational energies for the  \$B\ ^1\Sigma\_u^+\$ ,  \$c\ ^1\pi\_u\$ , and  \$a\ ^3\sigma\_g^+\$  states of the hydrogen molecule](#), J. Chem. Phys. **48**, 3672 (1968).
- [26] W. Kołos and L. Wolniewicz, [Theoretical investigation of the lowest doubleminimum state  \$e\$ ,  \$f\$ ,  \$^1\sigma\_g^+\$  of the hydrogen molecule](#), J. Chem. Phys. **50**, 3228 (1969).
- [27] W. Kołos, [Ab initio potential energy curves and vibrational levels for the  \$B''\$ ,  \$b\$ , and  \$b'\$  states of the hydrogen molecule](#), J. Mol. Spectrosc. **62**, 429 (1976).
- [28] W. Kołos and J. Rychlewski, [Ab initio potential energy curves and vibrational levels for the  \$C\$  and  \$D\ ^1\Pi\_u\$  states of the hydrogen molecule](#), J. Mol. Spectrosc. **62**, 109 (1976).
- [29] W. Kołos and J. Rychlewski, [Ab initio potential energy curves and vibrational levels for the  \$c\$ ,  \$l\$ , and  \$i\$  states of the hydrogen molecule](#), J. Mol. Spectrosc. **66**, 428 (1977).
- [30] L. Wolniewicz and K. J. Dressler, [The  \$B\ ^1\Sigma\_u^+\$ ,  \$B'\ ^1\Sigma\_u^+\$ ,  \$C\ ^1\Pi\_u\$ , and  \$D\ ^1\Pi\_u\$  states of the  \$H\_2\$  molecule. Matrix elements of angular and radial nonadiabatic coupling and improved ab initio potential energy curves](#), Chem. Phys. **88**, 3861 (1988).
- [31] G. Staszewska and L. Wolniewicz, [Adiabatic energies of excited  \$^1\Sigma\_u\$  states of the hydrogen molecule](#), J. Mol. Spectrosc. **212**, 208 (2002).
- [32] L. Wolniewicz and G. Staszewska, [Excited  \$^1\Pi\_u\$  and the  \$^1\Pi\_u \rightarrow X\ ^1\Sigma\_g^+\$  transition moments of the hydrogen molecule](#), J. Mol. Spectrosc. **220**, 45 (2003).
- [33] C. Lee, Y. Gim, and T. H. Choi, [Calculation of potential energy curves of excited states of molecular hydrogen by multi-reference configuration-interaction method](#), Bull. Korean Chem. Soc. **34**, 1771 (2013).
- [34] N. B. Oozeer, A. Ponra, A. J. Etindele, and M. E. Casida, [A new freely-downloadable hands-on density-functional theory workbook using a freely-downloadable version of DEMON2K](#), Pure Appl. Chem. **95**, 213 (2023).

- [35] M. E. Casida, [DEMON2K: Density-functional theory \(DFT\) for chemical physicists/physical chemists; Workbook number 1 \(Abrahams workbook\)](http://www.demon-software.com/public_html/tutorials/main.pdf), [http://www.demon-software.com/public\\_html/tutorials/main.pdf](http://www.demon-software.com/public_html/tutorials/main.pdf), 2022.
- [36] E. R. Davidson and D. Feller, [Basis set selection for molecular calculations](#), Chem. Rev. **86**, 681 (1986).
- [37] J. G. Hill, [Gaussian basis sets for molecular applications](#), Int. J. Quant. Chem. **113**, 21 (2013).
- [38] B. Delley, [An allelectron numerical method for solving the local density functional for polyatomic molecules](#), J. Chem. Phys. **92**, 508 (1990).
- [39] J. C. Slater, [Atomic shielding constants](#), Phys. Rev. **36**, 57 (1930).
- [40] G. te Velde, F. M. Bickelhaupt, E. J. Baerends, C. F. Guerra, S. J. A. van Gisbergen, J. G. Snijders, and T. Ziegler, [Chemistry with ADF](#), J. Comput. Chem. **22**, 931 (2001).
- [41] N. Godbout, D. R. Salahub, J. Andzelm, and E. Wimmer, [Optimization of Gaussian-type basis sets for local spin density functional calculations. Part I. Boron through neon, optimization technique and validation](#), Can. J. Phys. **70**, 560 (1992).
- [42] P. Calaminici, F. Janetzko, A. M. Köster, R. Mejia-Olvera, and B. Zuñ-Gutierrez, [Density functional theory optimized basis sets for gradient corrected functionals: 3d transition metal systems](#), J. Chem. Phys. **126**, 044108 (2007).
- [43] W. J. Hehre, R. Ditchfield, R. F. Stewart, and J. A. Pople, [Selfconsistent molecular orbital methods. IV. Use of Gaussian expansions of Slater-type orbitals. Extension to secondrow molecules](#), J. Chem. Phys. **52**, 2769 (1970).
- [44] P. C. Hariharan and J. A. Pople, [The influence of polarization functions on molecular orbital hydrogenation energies](#), Theor. Chim. Acta **28**, 213 (1973).
- [45] M. M. Francl, W. J. Pietro, and W. J. Hehre, [Selfconsistent molecular orbital methods. XXIII. A polarization-type basis set for secondrow elements](#), J. Chem. Phys. **77**, 3654 (1982).
- [46] R. Krishnan, J. S. Binkley, R. Seeger, and J. A. Pople, [Selfconsistent molecular orbital methods. XX. A basis set for correlated wave functions](#), J. Chem. Phys. **72**, 650 (1980).
- [47] F. Weigend and R. Ahlrichs, [Balanced basis sets of split valence, triple zeta valence and quadruple zeta valence quality for H to Rn: Design and assessment of accuracy](#), Phys. Chem. Chem. Phys. **7**, 3297 (2005).
- [48] N. Rega, M. Cossi, and V. Barone, [Development and validation of reliable quantum mechanical approaches for the study of free radicals in solution](#), J. Chem. Phys. **105**, 11060 (1996).
- [49] S. Huzinaga, [Gaussian-type functions for polyatomic systems. I](#), J. Chem. Phys. **42**, 1293 (1965).
- [50] G. C. Lie and E. Clementi, [Study of the electronic structure of molecules. XXI. Correlation energy corrections as a functional of the Hartree-Fock density and its application to the hydrides of the second row atoms](#), J. Chem. Phys. **60**, 1275 (1974).
- [51] A. J. Sadlej, [Medium-size polarized basis sets for high-level correlated calculations of molecular electric properties](#), Collection Czech. Chem. Commun. **53**, 1995 (1988).

- [52] J. Guan, P. Duffy, J. T. Carter, D. P. Chong, K. C. Casida, M. E. Casida, and M. Wrinn, [Comparison of local-density and Hartree-Fock calculations of molecular polarizabilities and hyperpolarizabilities](#), J. Chem. Phys. **98**, 4753 (1993).
- [53] R. Pu-Amérigo, M. Merchán, I. Nebot-Gil, P. Widmark, and B. O. Roos, [Density matrix averaged atomic natural orbital \(ANO\) basis sets for correlated molecular wave functions. III. First row transition metal atoms](#), Theor. Chim. Acta **92**, 149 (1995).
- [54] D. E. Woon and T. H. D. Jr., [Gaussian basis sets for use in correlated molecular calculations. V. Core-valence basis sets for boron through neon](#), J. Chem. Phys. **103**, 4572 (1995).
- [55] T. H. D. Jr., [Gaussian basis sets for use in correlated molecular calculations. I. The atoms boron through neon and hydrogen](#), J. Chem. Phys. **90**, 1007 (1989).
- [56] F. Jensen, [The basis set convergence of spin-spin coupling constants calculated by density functional methods](#), J. Chem. Theo. Comp. **2**, 1360 (2006).
- [57] T. H. Dunning and P. J. Hay, [Gaussian basis sets for molecular calculations](#), in *Methods of Electronic Structure Theory*, edited by H. F. S. III, volume 3 of *Modern Theoretical Chemistry*, page 1, Springer, 1977.
- [58] I. Cherkes, S. Klaiman, and N. Moiseyev, [Spanning the Hilbert space with an even tempered gaussian basis set](#), Int. J. Quant. Chem. **109**, 2996 (2009).
- [59] T. Ziegler, A. Rauk, and E. J. Baerends, [On the calculation of multiplet energies by the Hartree-Fock-Slater method](#), Theor. Chim. Acta **4**, 877 (1977).
- [60] B. Schaftenaar, [MOLDEN: A pre- and post processing program of molecular electronic structure](#), <https://www3.cmbi.umcn.nl/molden/>, Last accessed 22 May 2021.
- [61] G. Schaftenaar and J. H. Noordik, [MOLDEN: a pre- and post-processing program for molecular and electronic structures](#), J. Comput. Aided Mol. Des. **14**, 123 (2000).
- [62] G. Schaftenaar, E. Vlieg, and G. Vriend, [MOLDEN 2.0: quantum chemistry meets proteins](#), J. Comput. Aided Mol. Des. **31**, 789 (2017).